Attention Microfiche User,

The original document from which this microfiche was made was found to contain some imperfection or imperfections that reduce full comprehension of some of the text despite the good technical quality of the microfiche itself. The imperfections may be:

- missing or illegible pages/figures
- wrong pagination
- poor overall printing quality, etc.

We normally refuse to microfiche such a document and request a replacement document (or pages) from the National INIS Centre concerned. However, our experience shows that many months pass before such documents are replaced. Sometimes the Centre is not able to supply a better copy or, in some cases, the pages that were supposed to be missing correspond to a wrong pagination only. We feel that it is better to proceed with distributing the microfiche made of these documents than to withhold them till the imperfections are removed. If the removals are subsequestly made then replacement microfiche can be issued. In line with this approach then, our specific practice for microfiching documents with imperfections is as follows:

1. A microfiche of an imperfect document will be marked with a special symbol (black circle) on the left of the title. This symbol will appear on all masters and copies of the document (1st fiche and trailer fiches) even if the imperfection is on one fiche of the report only.

2. If imperfection is not too general the reason will be specified on a sheet such as this, in the space below.

3. The microfiche will be considered as temporary, but sold at the normal price. Replacements, if they can be issued, will be available for purchase at the regular price.

4. A new document will be requested from the supplying Centre.

5. If the Centre can supply the necessary pages/document a new master fiche will be made to permit production of any replacement microfiche that may be requested.

The original document from which this microfiche has been prepared has these imperfections:

☒ missing pages/figures numbered: 60 (& 4.2 in section 4).

☐ wrong pagination

☐ poor overall printing quality

☐ combinations of the above

☐ other

INIS Clearinghouse
IAEA
P. O. Box 100
A-1400, Vienna, Austria

B.A.R.C.-1114

B.A.R.C.-1114

भारत सरकार

GOVERNMENT OF INDIA

परमाणु ऊर्जा आयोग

ATOMIC ENERGY COMMISSION

RADIOCHEMISTRY DIVISION
ANNUAL PROGRESS REPORT FOR 1978

Edited by

M. S. Subramanian and Satya Prakash

भाभा परमाणु अनुसंधान केन्द्र

BHABHA ATOMIC RESEARCH CENTRE

बंबई, भारत

BOMBAY, INDIA

1981

B. A. R. C. -1114

B. A. R. C. -1114

GOVERNMENT OF INDIA
ATOMIC ENERGY COMMISSION

RADIOCHEMISTRY DIVISION
ANNUAL PROGRESS REPORT FOR 1978

Edited by

M. S. Subramanian and Satya Prakash

BHABHA ATOMIC RESEARCH CENTRE
BOMBAY, INDIA
1981

INIS Subject Category : B 13

Descriptors

BARC

RESEARCH PROGRAMS

RADIOCHEMISTRY

ACTINIDES

ACTINIDE COMPLEXES

SOLVENT EXTRACTION

QUANTITATIVE CHEMICAL ANALYSIS

ISOTOPE RATIO

FISSION YIELD

FISSION FRAGMENTS

FISSION PRODUCTS

RADIOCHEMISTRY DIVISION

ANNUAL PROGRESS REPORT FOR 1978

edited by

M.S. Subramanian and Satya Prakash

INTRODUCTION

1. This annual progress report of the Radiochemistry Division for 1978 forms the tenth in the series and in this report the R & D work is described under the headings Reactor Chemistry, Heavy Element Chemistry, Process Chemistry, Radioanalytical Chemistry & Services, Nuclear Chemistry and Instrumentation.

2. As part of work on the preparation of fuel materials by sol-gel process, microspheres of uranium oxide and uranium-thorium oxides were prepared in order to standardise methods for obtaining crackfree products of uniform shape, size and high density.

3. Basic research activities of the Division centred around studies on the chemistry of actinides and fission products. The vaporisation thermodynamics of compounds of Th and U were determined by transpiration and boiling temperature techniques. Uranium(III) sulphates and double sulphates were prepared and characterised by X-ray, thermal and infra-red analysis. Unusual complexes of Rh(0) and Rh(II) were stabilised in ammonium chloride single crystals for the first time and were studied by EPR to understand the nature of metal-ligand bonding.

4. The extraction of trivalent actinides and lanthanides by long chain amines from chloride solutions was studied. The extraction of actinides by long chain amines from carboxylate media indicated that uranium(VI) could be separated from all metal ions except Ag and Zr. A solvent extraction method for the separation of uranium and plutonium from wastes containing phosphoric acid was developed. The extraction of actinides by di-n-octyl-sulphoxide was investigated.

5. The mechanism of radiation chemical behaviour of U(VI) in hydrochloric and sulphuric acid media was established. Flash photolysis of aqueous potassium persulphate solution was carried out in order to study the spectral and kinetic behaviour of SO_4^- radical.

6. The work on process chemistry of neptunium was continued and studies were carried out on the use of primary and secondary amines for the purification and concentration of neptunium. The extraction behaviour of rare earths by TBP was investigated. The work on in-line instrumentation was continued and the gamma absorptiometer and colorimeter were tested for their reliability for in-line operation at the Fuel Reprocessing Division.

7. Studies were carried out on radiochemical, mass spectrometric and other analytical methods. A gamma spectrometric method was developed for the determination of isotopic composition of plutonium using low energy gamma rays of plutonium isotopes. A single stage anion exchange method for separation and purification of neodymium from fission products was developed for burn-up measurements. A method was standardized for the determination of isotopic abundances of uranium at nanogram level by thermal ionisation mass spectrometry. An electrophoretic method for deposition of actinides with high superficial density was developed in connection with the requirement of fissile targets to be used for relative power mapping during start up experiments of FBTR. A method was developed for extractive photometric determination Pu(IV) and Np(IV) present in mixtures.

8. Several aspects of nuclear fission such as charge distribution, mass distribution and fragment angular momentum in low energy fission of actinides

were studied. The studies highlight the role of shells and pairing effect on these distributions. Work was started on the development of fast methods of transportation of recoil products and radiochemical seperations with an aim to study the decay schemes of radionuclides relatively far removed from the line of stability. Half-lives of ^{232}U and ^{242}Pu were determined by combining alphaspectrometric and mass spectrometric techniques.

9. In addition to the basic and applied work described above, instruments needed for carrying out the R & D programmes of the Division were developed. A spark counting unit for counting fission tracks in thin plastic films was developed. An autoranging alpha level monitor to be used with fractionating column was developed. Fabrication and calibration of a remote pipetter for use in hot cells was completed. A versatile thermo-luminescence (TL) unit for glovebox operation was designed and fabricated.

10. The Division continued to provide mass spectrometric analyses to other Divisions in BARC and units of DAE. Several sources of actinide isotopes were supplied to other Divisions in BARC, other units of DAE and universities in the country. Training in nuclear and radiochemistry was provided to university students and teachers.

CONTENTS

1.1 Preparation of Fuel Materials by Sol-Gel Process

V.N. Vaidya, R.V. Kamat, J.K. Joshi, V.S. Iyer,
N.L. Srinivasan, K.T. Pillai and D.D. Sood

Work on the preparation of fuel materials in the form of microspheres by wet chemical route was continued by investigating the preparation of UO_2 and UO_2-ThO_2 microspheres, having a size of 500-700 micrometers, using the hydrolysis process[1]. During the year under report about 300 experiments have been conducted and in each experiment 50-70 g of uranium or uranium-thorium was used. The process parameters are being optimized, and reproducible batches having upto 99% yield of crack-free UO_2 microspheres have been made.

In the hydrolysis process precooled (0°) solution of uranyl nitrate is mixed with hexamethylenetetramine (hexa) and urea, and dispersed in the form of droplets in hot (90-95°C) geletion medium like paraffin oil or silicone oil. The droplets solidify into gelled microspheres in a few seconds and the meshed gel structure of hydrated uranium oxide entraps the left out reactants, products, and water. These microspheres are degreased with a suitable solvent like CCl_4 or C_2Cl_4, washed free of extra organic matter and salts, dried, calcined in air to U_3O_8, reduced with H_2 to UO_2 and sintered in argon and hydrogen atmosphere upto 1200°C to obtain high density ($>$98% T.D.) UO_2 microspheres. The main features for the process development were design of proper geletion columns, improvement of solution feeding system, development of washing and heating schemes, and the choice of proper feed composition. It was observed that the feed composition, particularly the metal ion content of the solution, has a significant effect on the overall process.

1.1.1 Uranium oxide Microspheres

The work on the thermal convection loop was discontinued since the UO_2 microspheres obtained by using this system did not have good shape (they were oblate), and gave a very poor percentage yield of crack-free sintered product.

To improve the shape of the microspheres a 70 cm tall glass column, externally heated by a nichrome tape heater, was filled with silicone oil (viscosity 100 centistoke at 25°C) and used for gelation of droplets. This oil has a viscosity of 35 cstk at 100°C, as compared to 10 cstk for paraffin and the higher viscosity helped in reducing the height of the gelation column as well as in improving the sphericity of the product. Simultaneously an automatic feed system was made for the improvement of the size distribution of the product. The system with the general gelation equipment is shown in Fig.1.

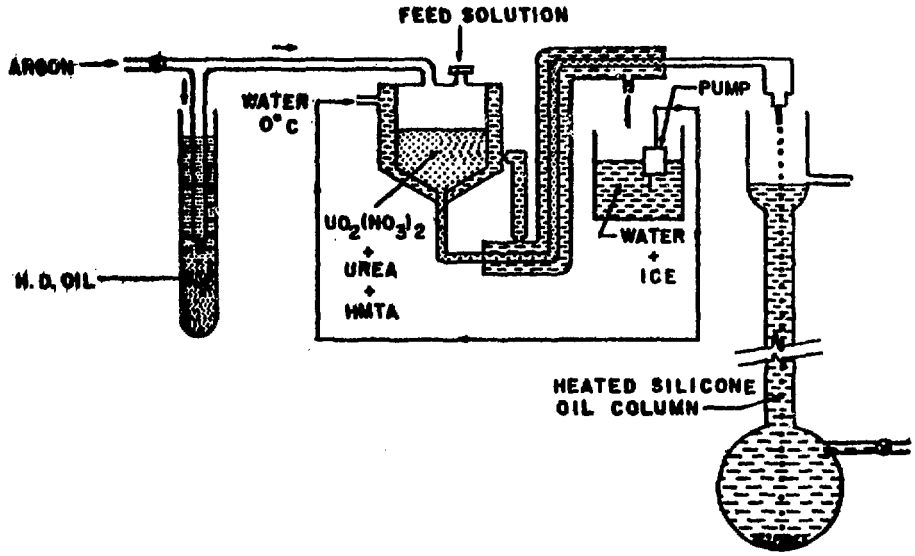

FIG. - 1.

General Gelation Equipment

The system consists of a double walled stainless steel tank, for containing the feed solution. The cold jacketted outlet of the tank is attached at the other end with capillary dispersers. A constant over pressure of gas in the tank produces droplets at the needle ends. The size of droplet depends on the overpressure of gas and the size of the capillary.

Fifty three experiments were carried out to prepare UO_{3-x} microspheres using this column. During these experiments the concentration of uranium was varied between 1.0 and 1.25 M, and the mole ratio [(hexa, urea)/U=R] was varied between 1.6 and 2.0. The gelled product was degreased by 4-6 washings with CCl_4, followed by air drying to remove CCl_4. The gel particles were then washed with hot (90-95°C) water and 12.5% NH_4OH solution. The washed microspheres were dried upto 100°C in 2 hours and then heated in air upto 500°C in 4 hours. The resultant product was UO_{3-x} gel microspheres. Out of 53 experiments only 28 batches gave 99% crack-free UO_{3-x} material. The feed composition for these good batches was [U] = 1.25 M and R = 1.8. The batches containing [U] = 1.1 M and R = 1.6 gave washed spheres which were too soft and formed clumps. The product from eight representative batches was sintered but only one of these gave 95% crack-free UO_2 microspheres whereas the rest of the batches failed badly and gave only 5 to 40% crack-free material. At this stage it was felt that a higher gelation time (> 25 s) may be necessary to obtain good quality spheres with silicone oil. For this purpose the length of the gelation column was increased from 70 cm to 165 cm to obtain gelation time of $\sim$ 50 seconds. With this column uranium concentration of 1.0 to 1.25 M and R = 1.4 was used in the feed solution. Higher values of R were not considered necessary with the longer gelation. The gelled microspheres were washed with 2.5% NH_4OH for 4 to 5 hours time. Different heating schemes were adopted. All the batches containing 1.25 M U in feed gave cracked product after sintering. The batches containing [U] = 1.0 M were too soft after washing and gave large clumps after washing and drying were completed.

With these results it was felt necessary to go back to the use of paraffin oil as gelation medium (250 cm tall column). During these experiments uranium concentration was varied from 0.75 M to 1.25 M and the ratio R from 1.4 to 2.0. As the uranium concentration was decreased the value of R was increased. For $[U]$ = 1.25 M, R was kept at 1.4, for $[U]$ = 1.1 M, R was 1.4 and 1.5 and for $[U]$ = 1.0 M, R was 1.5 and 1.6. Gelled spheres from these batches were washed in a glass column for 4 to 6 hours with 2.5% NH_4OH. The washed product was heated in air upto 500°C for 30 min followed by normal reduction sintering route. In many experiments (fifteen) where uranium in feed solution was 1.1 M and R = 1.5, more than 95% of UO_2 microspheres were crack-free. Batches starting with $[U]$ = 0.75 M and R = 2.0 gave soft gelled spheres difficult to handle but the final UO_2 product was 100% crack-free. All batches (six) containing $[U]$ = 1.0 M and R = 1.6 gave $>$ 98% crack-free UO_2 microspheres and the gelled spheres in these experiments did not pose any difficulty in handling. These experiments gave a clue that lower uranium concentration with high amount of urea and hexa ratio is more suitable for making UO_2 microspheres. These results were encouraging and it was decided to use the same procedure with 100 cstk silicone oil. The column was made 4 cm in diameter and 90 cm tall and a multiple nozzle (3 to 4 capillaries) system was used for feeding the solution. Wide column was aimed at preventing intercollision of spheres as well as improved thermal capacity for large feed rates. Using this column, fifty batches of UO_{3-x} microspheres were prepared. The feed composition used was $[U]$ = 1.1 M and R = 1.5 to 1.7. Three hours column wash with 2.5% NH_4OH solution was used, followed by drying at 100°C for 2 hours and calcination to 500°C in 20-25 minutes. The normal reduction, sintering route gave product with inconsistent results. About ten batches gave 95% crack-free product whereas the majority of batches failed. Further experiments were being carried out with $[U]$ = 1.0 M and R = 1.6 - 1.7 in the feed solution. The results of sintered product were encouraging as all batches gave $>$ 95% crack-free UO_2 microspheres.

These results indicate that a lower uranium molarity of feed composition, and higher ratio of urea and hexa, followed by fast calcination step gives a good product. Further work for establishing these points is in progress.

1.1.2 Uranium-Thorium Oxide Microspheres

Thirty batches of UO_2-ThO_2 microspheres containing 5-15% of Th were prepared using 250 cm tall glass column having paraffin oil and also using 70 cm tall column having 100 cstk silicone oil. All batches had used feed solution with metal content of 1.1 M and R = 1.5 - 1.7. The batches were washed using two routes i.e. hot water and 12.5 % NH_4OH solution or 2.5% NH_4OH solution. The product was heated upto 500°C at the rate of 300°C per hour and it was followed by reduction sintering. All batches gave better than 95% crack-free UO_2-ThO_2 microspheres with 95 to 97% theoretical density.

Reference

1. Radiochemistry Division Annual Progress Report for 1977, BARC - 1005 (1979)

SECTION 2 : HEAVY ELEMENT CHEMISTRY

2.1 Non-aqueous Chemistry

2.1.1 Vaporization Thermodynamics of Uranium Tetrafluoride

Rajendra Prasad, K. Nagarajan, M. Bhupathy, Ziley Singh, V. Venugopal and D.D. Sood

A number of investigators[1-4] have carried out vapour pressure measurements on solid UF_4 but there is a lack of agreement among the reported data. There is only one set of data[5] available for liquid UF_4 which is also in order to resolve the discrepancies two independent techniques, namely the boiling temperature and the transpiration have been used for vapour pressure measurement in the present study.

The vapour pressures determined by the boiling temperature and the transpiration methods for solid UF_4 can be represented by equations (1) and (2) and those for liquid UF_4 by equations (3) and (4) respectively.

$$\log_{10}(p/atm) = (10.15\pm0.25)-(16120\pm318)\ (K/T) \qquad (1)$$
(1246 to 1305 K)

$$\log_{10}(p/atm) = (9.79\pm 0.19)-(15714\pm239)\ (K/T) \qquad (2)$$
(1169 to 1307 K)

$$\log_{10}(p/atm) = (6.82\pm 0.25)-(11773\pm344)\ (K/T) \qquad (3)$$
(1312 to 1424 K)

$$\log_{10}(p/atm) = (7.23\pm0.3\ )-(12339\pm413)\ (K/T) \qquad (4)$$
(1318 to 1427 K)

These two sets of data agree with each other within 7% throughout the temperature range of investigation and hence were combined to give equations (5) and (6) for solid and liquid UF_4 respectively.

$$\log_{10}(p/atm) = (10.03\pm0.14)-(15994\pm716)\ (K/T) \qquad (5)$$

$$\log\ (p/atm) = (6.99\pm0.24\ )-(12014\pm335)\ (K/T) \qquad (6)$$

The present data for solid UF_4 agree excellently with those of Ryon and Twichell[1] and for liquid UF_4 agree with those reported by Langer and Blankenship[5]. The melting temperature of UF_4 calculated from equations (5) and (6) is 1309 K, which is in excellent

agreement with the directly measured value of (130±2) K[6]. The values of ΔH° (vap, 298 15 K) and ΔS°(vap, 298.15 K) calculated by the second law method are 77.8 Kcal mol^{-1} and 52.0 cal $K^{-1}mol^{-1}$ respectively.

Referemes

1. Ryon, A.D., Twichell, L.P., US report TL-7703 (1947)

2. Popov, M.M., Kostylov, F.A., Zubova, N.V., Russ. J. Inorg. Chem. 4, 770, (1959)

3. Akishin, P.A., Khodeev, Yu. Sr. Russ. J. Phys. Ch . 5, 574 (1961)

4. Chudinov, F.G., Chuprov, D.Ya, Russ. J. Phys. Chem. 44, 1106 (1970)

5. Langer, S., Blankenship, F.F., J. Inorg. Nucl. Chem. 14, 26 (1960)

6. Barton, C.J. Sheil, R.J., ORNL Unpublished data quoted in Reference (5)

2.1.2 Vaporisation Thermodynamics of Thorium Bromide

Ziley Singh, Rajendra Prasad, V. Venugopal, K.N. Roy and D.D. Sood

Vapour pressure of $ThBr_4$ has been reported only by Fischer et al[1]. In the present work the vaporisation behaviour of $ThBr_4$ has been studied to establish the data on this system using two independent techniques namely transpiration and boiling temperature.

The procedure for carrying out transpiration studies has already been reported earlier[2]. $ThBr_4$ used in the present work was prepared by reaction of Br_2 on ThH_4 at 500°K followed by vacuum distillation. The flow rate plateau obtained for $ThBr_4$ vapour was in the range of 2×10^{-5} to 8×10^{-5} m^3 min^{-1}. The vapour pressure data for the solid and the liquid are represented by equations (1) and (2) respectively.

$$\log (p/atm) = (10.54 \pm 0.11) - (11319 \pm 96) \ (K/T) \qquad (1)$$
(822 to 953 K)

$$\log (p/atm) = (6.84 \pm 0.16) - (7709 \pm 160) \ (K/T) \qquad (2)$$
(971 to 1068 K)

The apparatus and method used for the boiling temperature technique have been described previously[3]. The vapour pressure data for solid and liquid $ThBr_4$ obtained by this technique can be represented by equations (3) and (4) respectively.

$$\log (p/atm) = (10.65 \pm 0.13) - (11411 \pm 119) \ (K/T) \qquad (3)$$
(842 to 971 K)

$$\log (p/atm) = (6.94 \pm 0.12) - (7813 \pm 161) \ (K/T) \qquad (4)$$
(971 to 1089 K)

The vapour pressure data obtained by the two techniques agree within 2 per cent throughout the temperature range of measurements and hence the two sets of data were combined to give equations (5) and (6) which represent the vaporisation thermodynamics of $ThBr_4(s)$ and and $ThBr_4(l)$ respectively.

$$\log (p/atm) = (10.50 \pm 0.08) - (11357 \pm 69) \ (K/T) \qquad (5)$$

$$\log (p/atm) = (6.91 \pm 0.10) - (7779 \pm 110) \ (K/T) \qquad (6)$$

These equations were used to obtain melting temperature, normal boiling temperature, enthalpy of fusion and ΔH° (vap. 298.15 K) and the values are 970 K, 1127 K, 15.0 $Kcal_{th} mol^{-1}$ and 55.7 $Kcal_{th} mol^{-1}$ respectively.

For $ThBr_4(s)$ the present data are much lower than those of Fischer et al, but for $ThBr_4(l)$ the two sets of data are in good agreement. Since two independent techniques have been used during the present investigation and the results from both are in excellent agreement with each other, the present work can be considered as the best available data.

References

1. Fischer, W., Gewehr, R., Wingchen, H., Z. Anorg. All. Chem. 242 of 161 (1939)
2. Ziley Singh, Rajendra Prasad, V. Venugopal and D.D. Sood, J. Chem. Therm. 10, 129 (1978).

2.1.3 Transpiration and Boiling Temperature Studies on the Vaporisation Behaviour of Antimony

Rajendra Prasad, V. Venugopal, Ziley Singh and D.D. Sood

Vapour pressure of antimony has been measured by a number of workers, but there is discrepancy among these values particularly regarding the partial pressures of various species in the vapour phase[1]. In the absence of any consistent set of data, Hultgren et al[1] have estimated the vapour phase composition indirectly from other thermodynamic information. The vapour phase below 800 K consists almost entirely or Sb_4 molecules with Sb_2 and Sb species appearing at higher temperatures. The vapour phase concentration of antimony monomer is less than 0.5 per cent below 1300 K. In the present study the partial pressures of Sb (P_2°) and Sb_4 species (P_4°) have been determined in the temperature range of 1072 to 1265 K using an analytical method developed earlier[2]. The method uses the data on masses of antimony transported in experiments with antimony and an alloy of antimony under identical conditions. Transpiration studies on pure antimony, (0.40 Cu+0.60Sb) and (0.50 In+0.50Sb) alloys have been carried out for this purpose to obtain values of P_2° and P_4° from both alloy systems.

The total vapour pressure of antimony was also measured directly by boiling temperature method. Further, the transpiration and boiling temperature data on pure antimony were combined to calculate partial pressures of Sb_2 and Sb_4 species.

For pure antimony the mass (m°) of antimony transported per dm^3 of the carrier gas at 101.325 kPa pressure at 273.15 K can be expressed by equation (1)

$$\log_{10}(m^\circ/mg) = (7.33\pm0.07)-(6059\pm80)\ (K/T) \qquad (1)$$
$$(1076 \text{ to } 1265)$$

The mass of antimony (m) transported during studies on the liquid (0.40 Cu+0.60 Sb) alloy can be expressed by equation (2).

$$\log_{10}(m/mg) = (6.13\pm0.08)-(5625\pm89)\ (K/T) \qquad (2)$$
$$(1072 \text{ to } 1204 \text{ K})$$

Activity of Sb in the alloy was taken from Hultgren et al[3] and can be expressed by equation (3)

$$\log_{10} a_{Sb} = - 0.349 + 152.5 \ (K/T) \qquad (3)$$

The mass of antimony (m) transported during studies on the liquid (0.50 In + 0.50 Sb) alloy and activity of antimony in this alloy[3] can be expressed by equations (4) and (5).

$$\log_{10}(m/mg) = (6.33 \pm 0.20) - (6781 \pm 233) \ (K/T) \qquad (4)$$

(1125 to 1256 K)

$$\log_{10} a_{Sb} = - 0.383 - 73.02 \ (K/T) \qquad (5)$$

These data were used for obtaining the values for p_2° from (Cu+Sb) alloy as well as (In+Sb) alloy which could be represented by equations (6) and (7) respectively.

$$\log_{10}(p_2^\circ/kPa) = 4.73 - 6708 \ (K/T) \qquad (6)$$

$$\log_{10}(p_2^\circ/kPa) = 5.20 - 7274 \ (K/T) \qquad (7)$$

Similarly, the values of p° obtained from (Cu+Sb) and (In+Sb) system can be represented by equations (8) and (9) respectively.

$$\log_{10}(p_4^\circ/kPa) = 4.91 - 5992 \ (K/T) \qquad (8)$$

$$\log_{10}(p_4^\circ/kPa) = 4.84 - 5910 \ (K/T) \qquad (9)$$

The total pressure p obtained by combining dimer and tetramer partial pressures from (Cu+Sb) alloy and (In+Sb) alloy can be given by equations (10) and (11) respectively.

$$\log_{10}(p/kPa) = 5.09 - 6115 \ (K/T) \qquad (10)$$

$$\log_{10}(p/kPa) = 5.13 - 6179 \ (K/T) \qquad (11)$$

The total pressure was also directly measured by boiling temperature method and the data can be represented by equation (12)

$$\log_{10}(p/kPa) = (5.10 \pm 0.07) - (6149 \pm 84) \ (K/T) \qquad (12)$$

(1151 to 1263 K)

The values of p_2° and p_4° were also obtained by combining the boiling temperature data on total pressure with transpiration data given by equation (1) to obtain the average molar mass of the vapour and the mole fraction of dimer. These data can be represented by the following equations :

$$\log_{10}(p_2^\circ/kPa) = 6.37 - 8.796 \ (K/T) \qquad (13)$$

$$\log_{10}(p_4^\circ/kPa) = 4.51 - 5510 \ (K/T) \qquad (14)$$

The partial pressure of Sb (g) obtained from (Cu+Sb) and (In+Sb) alloys agree within 6 percent throughout the temperature range. Values of p_2° obtained by using the boiling temperature data agree with those from transpiration data within 18 per cent at 1200 K and within 2 per cent at 1300 K but at lower temperatures the agreement is poor. This is because at low total pressures a small error in the total pressure measurement results in a large error in the values of p_2°. Hence, the boiling temperature method is suitable only when the total pressure is large. In the case of $Sb_4(g)$ the partial pressures from the two alloy systems agree well within one per cent and within 10 per cent with the boiling temperature data. The data from the present investigation, however, do not agree with the values estimated by Hultgren et al.

Total pressure p obtained from (Cu+Sb) and (In+Sb) systems agree with the boiling temperature data within 3 per cent throughout the temperature range. The total pressure data also agree excellently with the values in the literature.

The standard enthalpy of vaporisation ΔH° (vap, 298.15 K) for dimer and tetramer species were calculated, by carrying out a third law analysis of the partial pressure data with the help of free energy functions of Sb(1), $Sb_2(g)$, $Sb_4(g)$ tabulated by Hultgren et al[1], and the values are 237.5 and 204.0 k J mol^{-1} respectively.

The partial pressure of antimony monomer (p_1°) has been evaluated using free energy functions of Sb(g) and $Sb_2(g)$ and the values of partial pressure and dissociation energy of $Sb_2(g)$. The free energy functions and the standard enthalpy of vaporisation of monomer were taken from Hultgren et al[1]. The values of p_2° and ΔH° (vap, 298.15 K) for dimer were taken from the present study. The values of p_1° thus calculated are represented by equation :

$$\log\ (p^\circ/kPa) = 7.56 - 12674\ (K/T) \qquad (15)$$

Some typical values of p_1° at 1100, 1200 and 1300 K are 1.1×10^{-4} 1.00×10^{-3} and 6.51×10^{-3} kPa. These data agree excellently with the data of Hultgren et al.

In conclusion, the values of p_2° and p_4° obtained from the two alloy systems bear excellent agreement with each other. The total pressure data calculated from these two alloy systems agree excellently with the total pressure data by boiling temperature method. The present data can therefore be taken to represent the vaporisation behaviour of antimony.

References

1. Hultgren, R., Desai, P.D., Hawkins, D.T., Gleiser, M., Kelley, K.K., Wagman, D.D. Selected Values of the Thermodynamic Properties of the Elements, American Society for Metals, (1973).
2. Prasad, R., Venugopal, V., Sood, D.D., J. Chem. Thermodynamics 9, 593. (1977)
3. Hultgren R., Desai, P.D., Hawkins, D.T., Gleiser, M., Kelley, K.K. Selected Values of the Thermodynamic Properties of binary alloys, American Society for Metals, (1973).

2.2 Structural Chemistry

2.2.1 X-ray Structural Studies

D.V. Srinivasan, A. Chadha, K.D. Singh Mudher, S.Sampath, K.L. Chawla, N.C. Jayadevan and D.M. Chakraburtty

2.2.1.1 Structure of $K_6(UO_2)_2(C_2O_4)_5.10H_2O$

The crystal structure of $K_6(UO_2)_2(C_2O_4)_5$ 10H O elucidated by us[1] on monolinic crystals with cell dimensions a=12.11A°, b = 9.98A°, C=9.34 A°, α = 92.6°, β = 101.2° and γ = 127.4° have been compared with the structure determined by Legros and Jeannin[2] on crystals with cell dimensions a = 10.103A°, b = 10.944A°, C.10.021A°, α = 121.4°, β = 104.7° and γ = 63.8°. The coordination of O atoms around the uranium atom, the nature of the different oxalate groups and the oxygen polyhedra around each K^+ ion are not significantly different in two structures.

2.2.1.2 Preparation and characterization of Uranium (III) sulphate and double sulphates

In continuation of our studies in uranium (III) complexes, uranium (III) sulphate, $U_2(SO_4)_3$ $8H_2O$, and its double salts $(NH_4)_2SO_4U_2(SO_4)_3.6H_2O$ $Rb_2SO_4.U_2(SO_4)_3.8H_2O$ and $Cs_2SO_4.U_2(SO_4)_3.11H_2O$ were prepared by the electrolytic reduction reported by Bernard et al (3) and characterised by x-ray thermal and IR methods, as detailed structural data on uranium (III) compounds are not yet available.

The compounds were precipitated from aqueous solution of uranium (III) obtained by the electrolytic reduction of ice cold uranyl sulphate solution under inert atmosphere. The dark olive green compounds were stored over P_2O_5 in argon filled desicator.

The x-ray powder pattern of $U_2(SO_4)_3.8H_2O$ indexed on an orthorhombic cell of dimensions a = 9.93 A°, b = 9.57°A° and c = 17.40 A° is given in Table 1. The pyucometric density of 3.41 g/ml showed 4 molecules to be present in a unit cell. The compound thus appears to be isostructural with $Ce_2(SO_4)_3.8H_2O$[4].

The x-ray patterns of the double sulphates are complex could not be indexed. Therefore only six of the strongest lines are listed in Table 2.

TABLE - 1

X-ray powder data of $U_2(SO_4)_3.nH_2O$ (λ = 1.5418 A°)

I/Io	2θ	d_{obs}	d_{cal}	hkl	I/Io	2θ	d_{obs}	d_{cal}	hkl
92	16.36	5.416	5.402	112	17	42.54	2.125	2.1267	316
13	17.76	4.989	4.965	200	29	43.20	2.094	2.097	136
13	18.50	4.754	4.785	020	8	43.74	2.0695	2.074	118
8	19.20	4.621	4.614	021	21	45.62	1.9885	1.992	208
63	20.42	4.349	4.350	004	29	45.90	1.977	1.980	028
13	24.18	3.681	3.678	114	13	47.02	1.933	1.933	511
			3.691	023	13	47.90	1.899	1.898	512
17	25.74	3.461	3.446	220	26	49.66	1.836	1.837	152
13	27.26	3.271	3.272	204	13	50.74	1.799	1.8006	336
50	27.70	3.220	3.219	024	8	53.30	1.719	1.725	154
21	28.78	3.102	3.106	115	34	54.54	1.683	1.686	227
39	30.26	2.944	2.962	223	8	55.54	1.654	1.655	600
34	31.14	2.872	2.867	132				1.654	155
42	33.22	2.697	2.700	224	8	56.34	1.633	1.636	408
			2.691	133	4	57.06	1.614	1.615	516
100	33.62	2.666	2.673	116	8	58.50	1.5777	1.577	156
26	40.62	2.221	2.187	226	13	59.86	1.545	1.547	604
			2.221	332	4	60.54	1.529	1.531	248
26	40.94	2.204	2.204	420					
21	41.62	2.169	2.175	008					
17	41.90	2.156	2.156	240					
			2.156	404					

TABLE - 2

X-ray powder data of $M_2SO_4 \cdot U_2(SO_4)_3 \cdot nH_2O$ ($\lambda = 1.5418$ A°)

(six strongest lines)

M = Rb^+ n=8		M = NH_4^+ n=8		N = Cs^+ n=11	
I/I_o	d_{obsd}	I/I_o	d_{obsd}	I/I_o	d_{obsd}
85	6.417	100	6.417	95	6.467
100	3.497	45	4.760	70	4.185
70	3.179	73	3.220	95	2.985
70	2.987	26	2.986	100	2.377
70	2.724	27	2.380	75	2.157
95	2.143	38	2.149	70	2.145

TABLE - 3

Thermal Behaviour of Uranium (III) Complexes

Compound	Atmosphere	Temperature	Product
1. $U_2(SO_4)_3.8H_2O$	Air	350°C	$U_2(OH)_2(SO_4)_3$
		650°C	$UO_2(SO_4)$
		800°C	U_3O_8
	Hydrogen	800°C	UO_2
2. $(NH_4)_2SO_4.U_2(SO_4)_3.8H_2O$	Air	650°C	UO_2SO_4
		900°C	U_3O_8
	H_2	200°C	$(NH_4)_2.SO_4.U_2(SO_4)_3$
		800°C	UO_2
3. $Rb_2SO_4.U_2(SO_4)_3.8H_2O$	Air	incomplete	decomposition upto 900°C
	Argon	950°C	$Rb_2U_2O_7$
	Hydrogen	200°C	$Rb_2(SO_4).U_2(SO_4)_3$
		800°C	UO_2 (incomplete for mation)
4. $Cs_2SO_4.U_2(SO_4)_3.11H_2O$	Air	600°C	$Cs_2(UO_2)_2(SO_4)_3$
		1000°C	$Cs_2U_2O_7$ (incomplete formation
	Argon	Argon 900°C	$Cs_2U_4O_{12}+UO_2$
		1000°C	UO_2
	Hydrogen	800°C	UO_2

The thermal decomposition of the compounds in air, argon and hydrogen was studied on a Mettler Thermoanalyser. The results are collected in Table 3 giving the final decomposition products and the intermediate stable phases isolated, if any, along with the temperatures.

The formation of UO_2 by thermal decomposition of U(III) compounds in hydrogen indicates the possibility that water molecules coordinated to the uranium atom is responsible for the oxidation of uranium (III). The IR spectra of U(III) compounds indicate co-ordination of water molecules.

2.2.1.3 Cs-U-Pu-O system - Phase Studies

Reduction of $Cs_2U_2O_7$ with hydrogen in the range of 600-700°C for about 70 hours gave a new phase along with UO_2. The x-ray pattern of the new phase could be indexed on an orthorbombic cell with a = 4.12 A°, b = 6.58 A° and c = 5.83 A°. Since the reduction of other alkali metal diuranates $M_2U_2O_7$ with hydrogen is known to give MUO_3[5], the new phase is most probably $CsUO_3$. Experiments to confirm the composition are in progress.

Reaction of Cs_2CO_3 with a mixture of UO_2 and 30% PuO_2 or with its MO_2 solid solution gave a mixture of PuO_2 and caesium uranates. $Cs_2(U,Pu)O_7$ is the only phase containing plutonium.

References

1. Annual Report (1977), Radiochemistry Division, BARC
2. P.J. Legros and Y.Jeannin, Acta, Cryst. B32, 2497 (1976)
3. Bernard et al. JCS(Dalton), 1964, (1972)
4. G.Pennetier and A. Dereigre, Bull. Soc. Chem. France 1, 102 (1965)
5. S.Kemmler - Sack and W. Rudorff, 7, Anorg. Allg. Chem., 354, 255 (1967)

2.2.2 Electron Paramagnetic Resonance of Rh° and Rh^{2+} in NH_4Cl Single Crystal

M.D. Sastry, K. Savitri and B.D. Joshi

The electron paramagnetic resonance (EPR) study of gamma-irradiated ammonium chloride single crystals doped with diamagnetic Rh^{3+} has indicated the presence of two paramagnetic centres identified as Rh° ($4d^9$) and Rh^{2+} having low spin configuration in compressed octahedral coordination. Figure 2 shows the spectrum obtained in gamma-irradiated Rh: NH_4Cl at room temperature and at liquid nitrogen temperature. Lines marked Centre I, are due to Rh^{2+} and those marked centre-II are due to Rh°. The EPR spectrum of Rh° has been found to be highly temperature dependent, the intensity increasing with decreasing temperature, and was observable only below 173°K . The unpaired electron is in 'pure' $|3\,s^2-r^2\rangle$ orbital and a small temperature dependent orthorhombic distortion suggests the probable coupling of $|3\,s^2-r^2\rangle$ state with Q_2-type of normal mode of vibration. Furthermore, the hyperfine structure of neutral

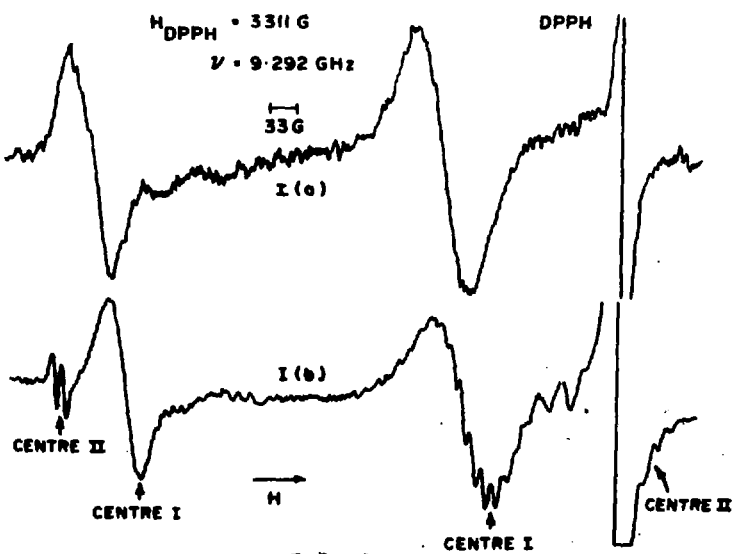

FIG.-2.

EPR Spectrum of Gamma Irradiated Rh: NH_4Cl

rhodium atom in solid state has been observed at room temperature and the g-values suggest the predominant $|x^2-y^2\rangle$ character of the unpaired electron. At temperatures lower than 120K super-hyperfine structure due to ligand Cl^- ions has been observed and it elucidates the nature of metal-ligand bonding for Rh^{2+} complex.

2.3 Thermal Studies

P. Anandakumaran, R.K. Swamy, Hita Hadap, R.R. Khandekar, N.C. Jayadevan and D.M. Chakraburtty

2.3.1 Oxidation of 30% PuO_2-UO_2 Sintered Pellets

To dertermine the compositions of the orthorhombic and cubic phases formed in the oxidation of PuO_2-UO_2 solid solution, the following experiments were done on sintered 30% PuO_2-UO_2 pellets. A typical set consisted of :

(i) equilibration of the pellet to form $MO_{2.000}$

(ii) oxidation in a slow stream of air upto 460°C to obtain the maximum O/M of 2.385,

(iii) extraction of the oxidised product with 15 ml portions of 0.35N HNO_3, to remove the M_3O_8 formed,

(iv) Reduction of the dried residue to $MO_{2.000}$ followed by oxidation in air upto 460°C to obtain the maximum O/M of 2.270, and

(v) dissolution of the product in HNO_3+HF mixture.

All the M_3O_8 phase formed at 460°C could be extracted with about 100 ml. of 0.35N HNO_3 leaving the cubic phase unaffected. The results are shown in Table 4 as the average of 4 experiments each. In a typical set, 8.210 mg Pu and 154.34 mg U were extracted from 1.27205 g of $MO_{2.380}$ while 1.06435 g of the residue had 320.86 mg Pu and 606.08 mg U.

The air oxidation of 30% PuO_2-UO_2 solid solution thus results in two phases, an orthorhombic $(U_{0.95}Pu_{0.05})O_{8-z}$ phase and a cubic $(U_{0.65}Pu_{0.35})O_{2.27}$ phase.

2.3.2 Kinetics of Oxidation of Uranium Monocarbides

The kinetics of Oxidation of Uranium Monocarbide was followed gravimetrically using the Mettler Thermoanalyser to study the mechanism of oxidation.

Table - 4

Chemical Analysis Results

No.	Sample Description	O/M before dissolution[a]	$\frac{Pu}{Pu + U}$
1.	Original pellet dissolution HNO_3- HF	2.000	0.299[b]
2.	0.35 N HNO_3 extract of sample	2.385	0.052[c]
3.	Residue from No.2 dissolved in HNO_3- HF	2.270	0.346[b]

Precision for the estimations (1σ)

a : 0.005

b : Pu-0.2%; U-0.2%

c : Pu-0.8%; U-0.5%

Uranium monocarbide samples obtained from AFD, BARC were powdered in argon atmosphere and heated in flowing dry air at the rate of 10°C/minute. The thermogram showed that weight gain started from 180°C onwards with a point of inflection at 410°C. The kinetic parameters for the oxidation reaction from 180°C to 410°C were calculated by the difference-differential method using Freeman and Carrol equation. The percentage weight gain with respect to the initial sample weight and α, the fractional conversion with respect to the total weight gain are given in Table 5. A straight line plot of log $g(\alpha)$ against temperature was obtained in Figure 3 if $f(\alpha) = (1-\alpha)^n$ with n=1 indicating that the rate of oxidation is controlled by the random nucleation of the products of oxidation[1].

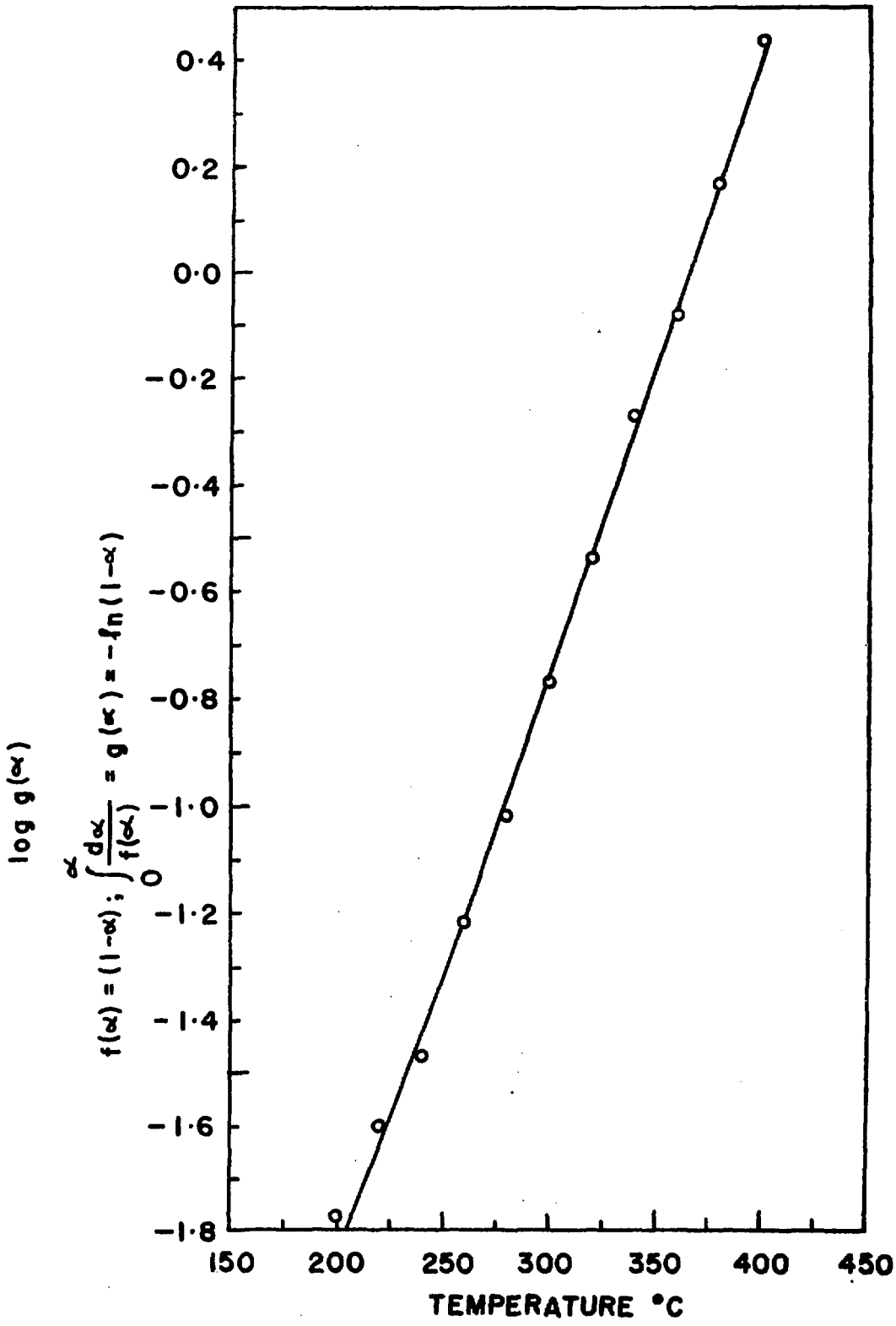

FIG. - 3. A Plot of log g (α) Vs Temperature

TABLE - 5

No.	Temp.°C	Fractional Conversion (α)
0	180	0.0000
1	200	0.0167
2	220	0.0250
3	240	0.0333
4	260	0.0583
5	280	0.0917
6	300	0.1583
7	320	0.2500
8	340	0.4167
9	360	0.5667
10	380	0.7667
11	400	0.9333
12	410	1.0000

The Freeman-Carroll plot in Figure (4) showed the oxidation reaction to follow first order kinetics with an activation energy of 21.68 kcal/mole.

The total weight gain of 3.5% upto 410°C attributed to a phase UCO_{1-x} where x = 0.45.

REFERENCES

1. Sestak. Thermal Analysis "Ed. Wilderman, 2, 24 (1971)

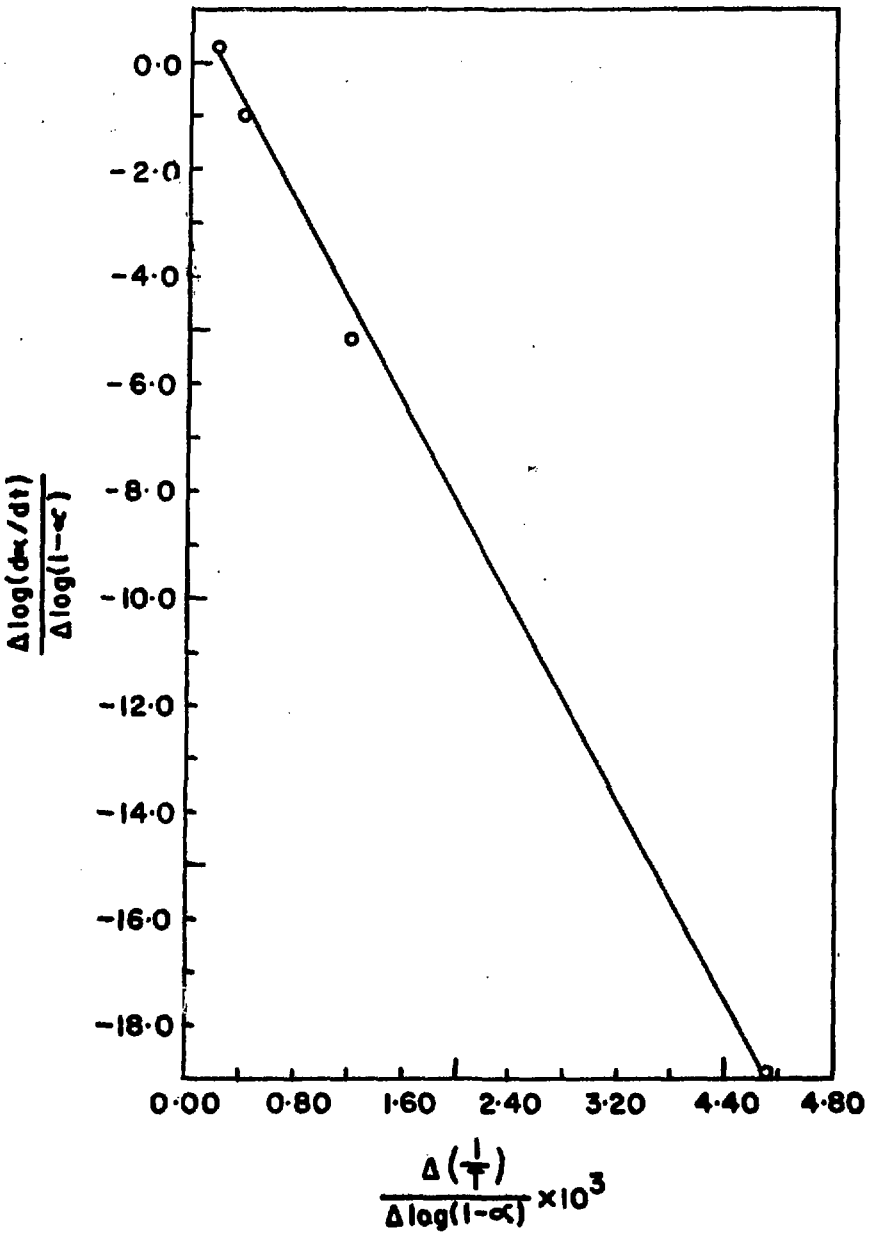

FIG.- 4.

The Freeman - Carroll Plot

2.4 Solvent Extraction and Ion-exchange Studies

2.4.1 Solvent Extraction of Actinides and Fission Products by Long Chain Sulphoxides

S.A. Pai, J.P. Shukla and M.S. Subramanian

In continuation of our investigation on extraction by long chain sulphoxides, the solvent extraction of actinides and some fission products by di-n-octyl sulphoxide has been investigated.

Di-n-octylsulphoxide (DOSO) has been synthesised by a two step process. The oxide product was recrystallised from petroleum ether (60-80°) to give white crystals (155 g) m.pt 75°C, C = 70.1%, H = 12.3%, S = 11.8% required for $(C_8H_{17})_2SO$, C = 70.44%, H = 12.4%, S = 11.7%.

The extraction behaviour of plutonium(IV), uranium(VI) and some fission products like ^{95}Zr, $^{103,106}Ru$, ^{144}Ce, $^{152,154}Eu$ and ^{90}Sr from nitric acid media by DOSO in Solvesso-100 has been investigated over a wide range of conditions. Whereas the actinides are extracted essentially completely, the fission products show negligible extraction. The absorption spectra of sulphoxide extracts containing either Pu^{4+} or UO_2^{2+} indicate the species extracted to be disolvates. DOSO extracts actinides better than di-hexylsulphoxide (DHSO) under all conditions and is also more soluble in aromatic diluents than the latter. This is in keeping with its higher basicity.

2.4.2 Synergistic Solvent Extraction Studies

S.K.Patil, V.V.Ramakrishna, A.Ramanujam*, B.Haraprakas* and K.M. Gudi

The synergistic extraction of Pu(IV) by mixtures of HTTA (thenoyltri-fluoroacetone) and TBP (tri-n-butylphosphate) in benzene from perchloric acid medium showed the formation of the adduct $Pu(TTA)_4.TBP$ The adduct formation was also studied by spectrophotometry. Values of the equilibrium constants obtained are given in Table 6.

---

*Fuel Reprocessing Division, BARC

Table - 6

Summary of equilibrium constants for the adducts of U(IV), Np(IV) and Pu(IV) β-diketonates with some neutral donors

Adduct	Neutral ligand(S)	Diluent	log K_A	log $_{AB}$	log K_{AB}
$U(TTA)_4.S$	TOPO	Benzene	5.42	6.23	11.65
	EBPO	"	5.42	6.13	11.55
	TPPO	"	"	4.72	10.14
	TBBP	"	"	4.04	9.46
	TBP	"	"	3.04	8.46
	TIOTP	"	"	1.27	6.69
	MIBK	"	"	-0.10	5.32
	TOPO	Chloroform	-	3.98	-
$Np(TTA)_4.S$	TBP	Cyclohexane	6.29	4.23	10.52
$Pu(TTA)_4.S$	TBP	Benzene	7.34	1.70	9.04

The extraction of Np(IV), by mixtures of HTTA and TBP in cyclohexane from perchloric acid medium, was investigated and the complex $Np(TTA)_4$. TBP was found responsible for the observed synergism. The respective equilibrium constants obtained are also included in Table 6.

Formation of adducts between $U(TTA)_4$ and several neutral donors (S) was investigated by spectrophotometry. Typical spectra of $U(TTA)_4$ and $U(TTA)_4$. S, present in different compositions are given in Fig. 5. The composition of the adducts was derived from the plots of absorbance vs. $[S] / [U(IV)]$, a typical plot being shown in Fig. 6. Values of the equilibrium constants obtained are summarised in Table 6.

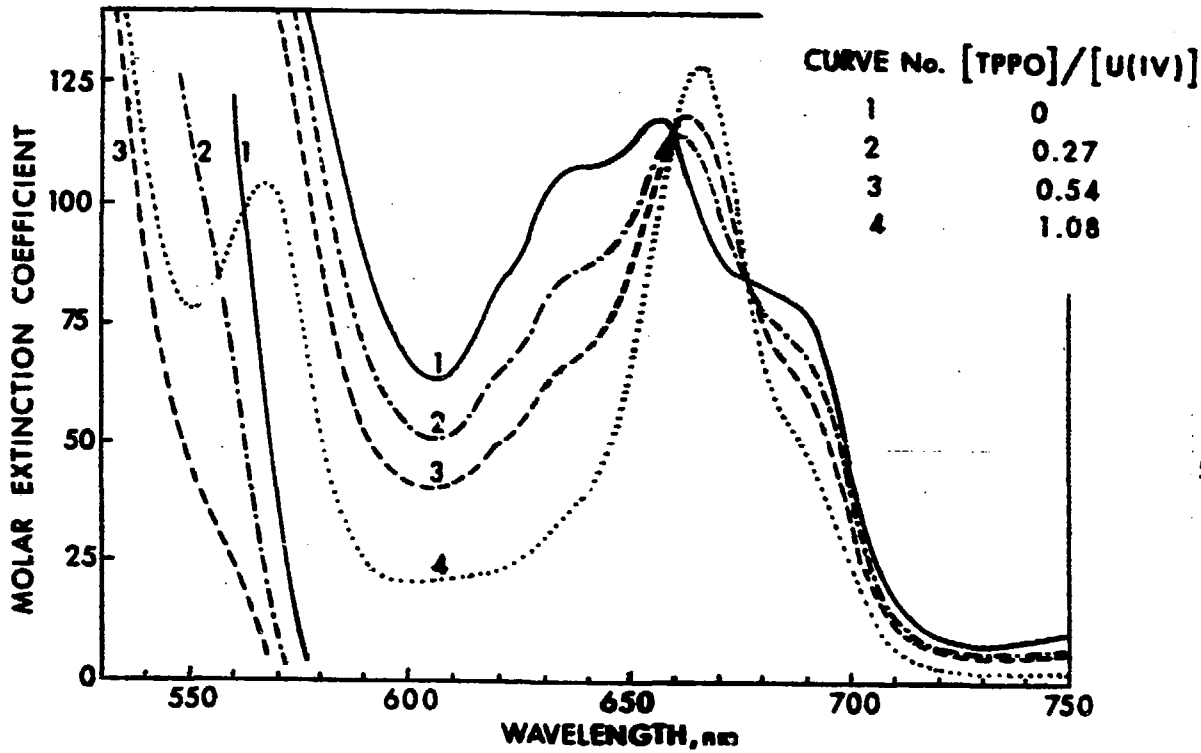

FIG.-5.

A Plot of Molar Extinction Coefficient for Different $[TPPO]/[U(IV)]$ Ratio VS Wavelength.

It was established that synergism in tetravalent actinides is a consequence of the increase in coordination number from 8 to 9 in their adducts with neutral donors. It was also shown that the solubility of water in organic solvents is not a major factor, if at all, contributing to the destruction of synergism.

The adduct formation between $UO_2(TTA)_2$ and the neutral donors TOPO and DBBP was investigated by spectrophotometry. The changes in the absorption spectrum of $UO_2(TTA)_2$ due to addition of TOPO are shown in Fig.7. The presence of isobestic points suggest the presence of only two absorbing species. The changes in absorbance at different wavelengths for different $[TOPO]$ / $[U(VI)]$ ratios is shown in Fig.8. A clear break at $[TOPO] : [U(VI)] = 1$ shows that the adduct formed has the composition $UO_2(TTA)_2TOPO$. Similarly with DBBP, $UO_2(TTA)_2DBBP$ was found to be formed.

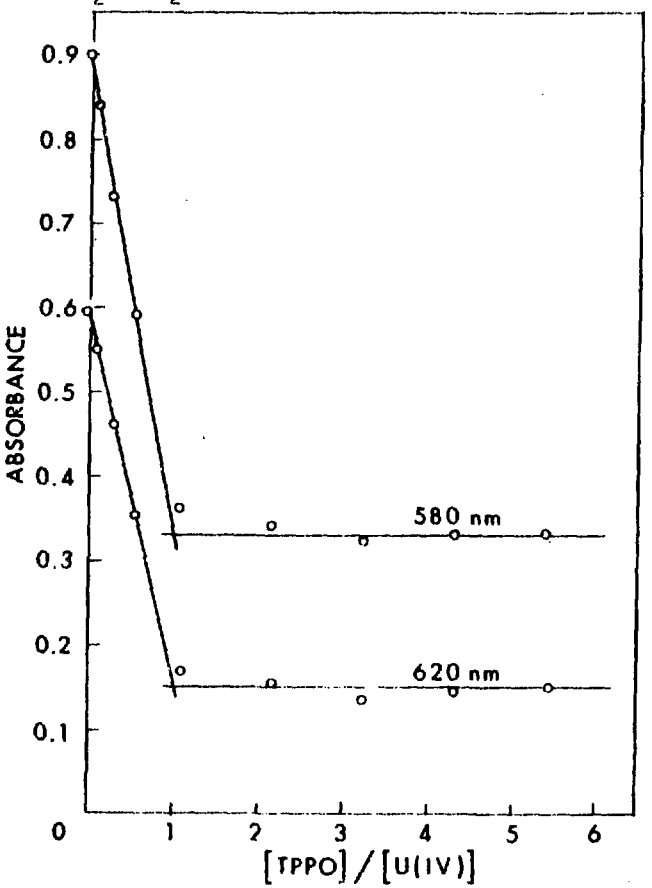

FIG. - 6.
A Plot of Absorbance VS $[TPPO]$ / $[U(IV)]$

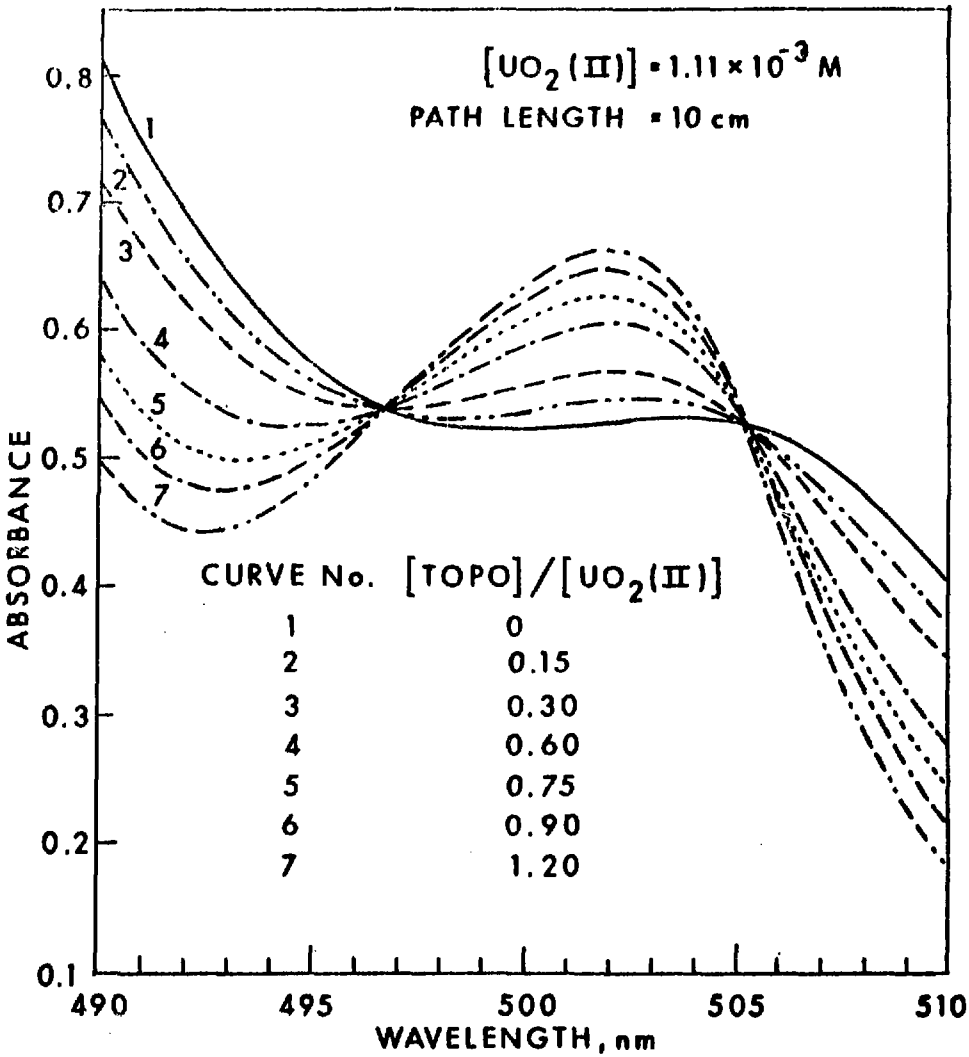

FIG.-7.

Absorbance for different [TOPO] / [UO_2(II)] Ratios VS Wavelength

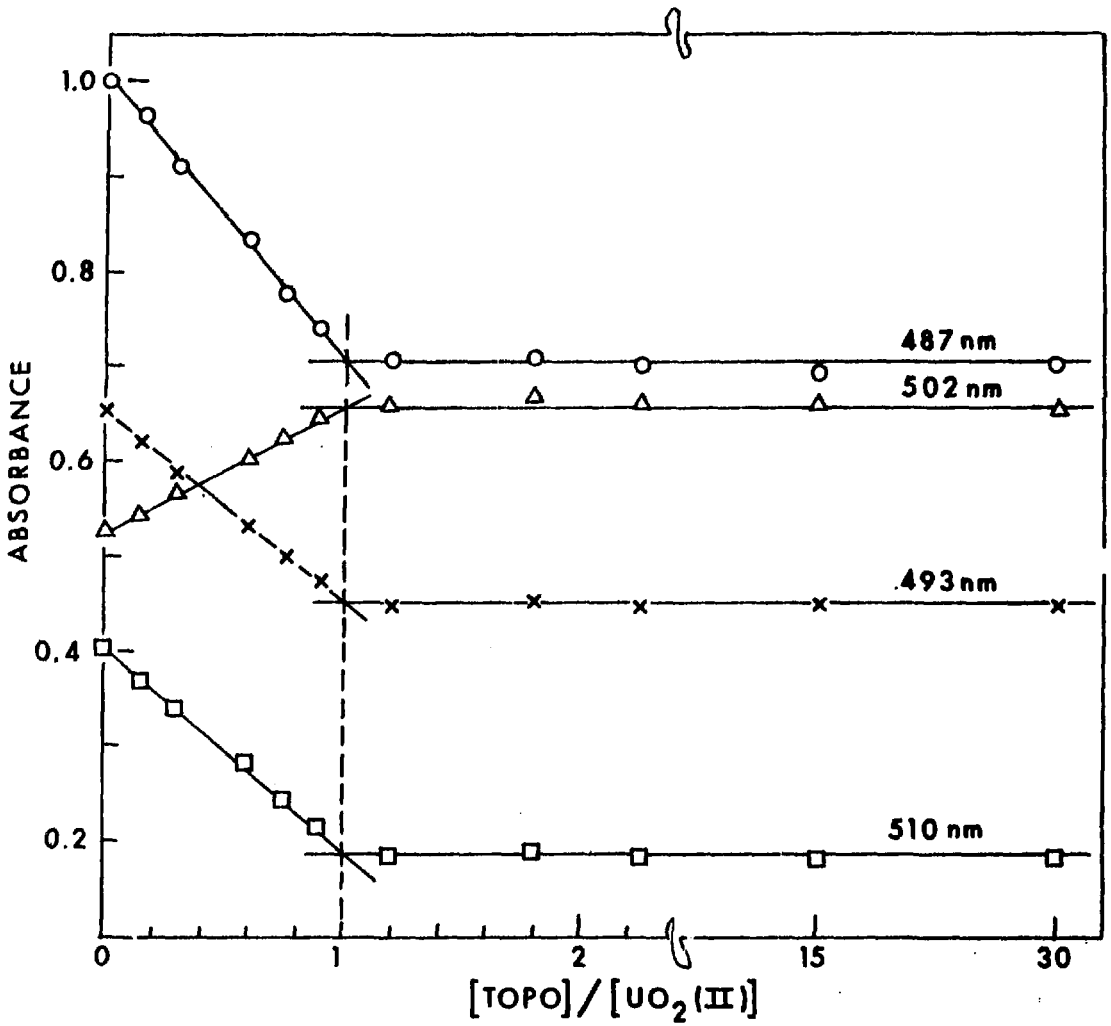

FIG.- 8.

A Plot of Absorbance VS $\frac{[TOPO]}{[UO_2(II)]}$

2.4.3 Extraction of Actinides by Long-Chain Amines

S.K. Patil, Veena Bhandiwad and Rajendra Swarup

2.4.3.1. Separation Studies from Carboxylate Media

An exploratory work was carried out to develop a method for the separation of U(VI) from aqueous malonate medium by extraction from amines. The distribution coefficient data for the extraction of different metal ions by 20% TIOA in xylene from an aqueous mixture of 1M malonic acid +0.25M nitric acid were obtained and are summarised in Table 7. The data suggest that U(VI) can be separated satisfactorily from all the metal ions tried except Ag and Zr.

Table 7

Distribution Coefficient of U(VI) and some metal ions by 20% TIOA in xylene from malonic and nitric acids mixture.

Aq. phase - 1M malonic acid + 0.25M nitric acid

Metal ions tracer	K_d
U	17
Ag	3.5
Zr	0.35
Cs	1.25×10^{-2}
Co	1.5×10^{-3}
Zn	5.5×10^{-4}
Eu	1.4×10^{-4}
Tb	7.5×10^{-5}

2.4.3.2. Effect of temperature on the extraction of Np(IV) from TLA Solvesso-100 from nitric acid

The effect of temperature on the extraction of Np(IV) from aqueous nitric acid by TLA was studied. Distribution coefficient data obtained at different temperatures are summarised in Table 8. It is seen from the data that the K_d values of Np(IV) decrease with increasing temperature. The equilibrium concentration of nitric acid in the TLA phase as a function of temperature remained almost constant. The enthalpy values calculated from the plots of log K_d vs 1/T are included in the Table 8 which show that the ΔH values increase with increasing concentration of amine.

Table 8

Distribution Coefficient of Np(IV) between nitric acid and TLA-Solvesso-100 as a function of temperature

HNO_3 (M)	TLA Vol.%	Distribution Coefficient (K_d) 20°C	30°C	40°C	50°C	60°C	$-\Delta H$ Kcal/mole
2	1	0.36	0.22	0.14	0.094	0.061	8.60
	5	8.2	5.44	3.6	2.2	1.47	8.42
	10	32.5	20.9	14.2	10.4	7.37	7.12
4.	1	0.46	0.28	0.184	0.12	0.082	8.51
	5	9.23	6.6	4.25	2.81	1.94	8.03
	10	36.2	25.8	16.32	11.12	7.76	7.63

2.4.4 Extraction of Trivalent Actinides and Lanthanides by long Chain Amines from Concentrated Chloride Solutions

P.K. Khopkar and Jagdish N. Mathur

The present work deals with the extraction of Am(III) and Eu(III) - which represent the trivalent actinides and lanthanides respectively - by primary, secondary, tertiary and quaternary amines

in xylene medium from concentrated lithium chloride solutions of low acidities. Absorption spectra of Am(III) extracted by tertiary and quaternary amines from concentrated lithium chloride have been studied in order to elucidate the nature of the Am(III) species extracted by these extractants.

The primary and the secondary amines used were Primene-JMT and Amberlite-LA1 respectively. These as well as the tertiary and quaternary amines TICA, TnOA, Alamine-336, TLA, Aliquat-336 and ThpACl were used as received from commercial sources. All the amines except the quaternary ones were converted into their hydrochlorides by equilibrating their xylene solutions with 1 N HCl. The amine solutions were then preequilibrated with conc. LiCl (pH = 2.0). The tracers ^{241}Am and $^{152,154}Eu$ were radiochemically pure. Solvent extraction experiments were carried out using 0.2, 0.15 and 0.10 M solutions of the amines in xylene, the equilibration time being 15 minutes. Radioassay of the tracers was done using a NaI(Tl) well-type scintillation counter. Absorption spectra were recorded using Cary-14 absorption spectrophotometer. Oscillator strengths were calculated using the method of Carnall et al[1].

Extraction data for Am(III) and Eu(III) using the tertiary and quaternary amines and the separation factors obtained are presented in Table 9. Though negligible ($k_d < 10^{-3}$) extraction of both Am(III) and Eu(III) was observed with primary and secondary amines, the tertiary and quaternary amines showed appreciable extraction of both Am(III) and Eu(III) under these conditions, the trivalent actinides always showing a higher extraction.

Extraction of trivalent actinide and lanthanide chloro complexes by tertiary and quaternary amines can be represented by reactions (1) and (2).

$$MCl_3 + Y\,(R_3NH\,Cl)_{m\,org} \longrightarrow MCl_{3+mY}\cdot mYR_3NH_{org} \quad \ldots\ldots (1)$$

$$MCl_{3\,aq} + Z(R_4NCl)_{n\,org} \longrightarrow MCl_{3+nZ}\cdot nZ\cdot R_4N_{org} \quad \ldots\ldots (2)$$

where m and n are the degrees of polymerization of the tertiary and the quaternary amines respectively. As seen from Table 9 the separation

factors obtained when tertiary amines are used as extractants are as a class far higher than those obtained using the quaternary amines though differences do exist in the separation factors obtained using various amines of the same class.

Table - 9

Extraction of Am (III) and Eu (III) by tertiary and quaternary amines

Amine	Conc. M	Distribution Coefficient K_d		S.F. $\frac{K_d}{K_d}$
		Eu(III)	Am(III)	$\frac{Am}{Eu}$
Tetraheptyl ammonium Chloride	0.10	27.88	68.70	2.5
	0.15	43.54	111.90	2.6
	0.20	55.95	150.70	2.7
Aliquot chloride	0.10	1.98	8.97	4.5
	0.15	2.70	12.53	4.7
	0.20	3.34	16.34	4.9
Alamine-336	0.10	0.008	0.289	37.2
	0.15	0.015	0.670	43.8
	0.20	0.032	1.480	46.0
Tri-iso-octyl Amine	0.10	0.013	0.850	63.9
	0.15	0.034	2.147	63.3
	0.20	0.053	3.303	62.4
Tri-n-octyl Amine	0.10	0.008	0.496	59.7
	0.15	0.026	1.460	55.3
	0.20	0.052	2.891	55.8
Trilauryl Amine	0.10	0.006	0.329	54.0
	0.15	0.013	0.764	57.4
	0.20	0.020	1.183	58.3

In a comprehensive study of the nature of the anionic chloro complexes of U(IV), U(VI) and other metal ions Ryan has demonstrated[2] the role of hydrogen bonding in stabilization of the hexachloro-and

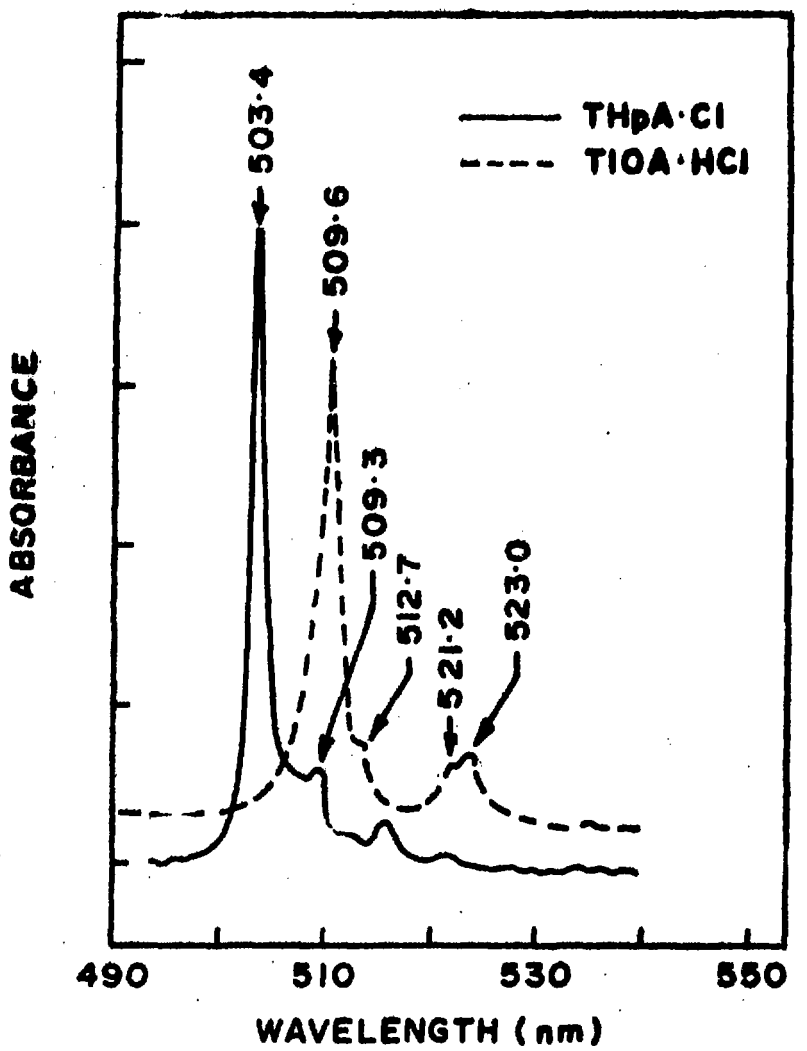

FIG. - 9.

Amine Extraction of Am(III) - Chloro Complexes in Xylene

the tetrachloro complexes when either the tertiary amines or anion-exchange resins in conjuction with hydronium ions were used. It is quite conceivable that in the case of trivalent actinide and lanthanide chloro complexes also, hydrogen bonding may play an important part. Obviously such a bonding could come into play only when tertiary amines (with the R_3NH^+ cation) are used as extractants. In a study of thiocyanate complexes of Am(III) extracted into the organic phase, Khopkar and Mathur[3] have shown that the extent of covalency in the Am(III)-thiocyanate bonds increases as the number of thiocyanate ligands attached to Am(III) increases, as a result of increased ligand field of thiocyanate ions. It looks quite likely therefore that with the stabilization of higher chloro complexes through hydrogen bonding with the cation of the tertiary amines the covalency in the Am(III)-chloride bonds and hence the stability of these complexes is enhanced with respect to that for Eu(III)-chloro complexes. It is well known that covalent bonds in the latter case are ruled out due to the '4f' electrons being well shielded as compared to '5f' electrons which extend appreciably in space[4].

Absorption spectra of Am(III) extracted by two representative amines, the tertiary amine TIOA.HCl and the quaternary amine ThpACl are presented in Fig.9. Details of the absorption spectral parameters of Am(III) extracted by several amines are given in Table 10.

In order to examine this problem further, absorption spectra of the chloro complexes of Am(III) extracted by the two classes of amines were investigated in the region of the 503 nm band which is ascribed to the first excited level $^7F_0 \rightarrow {}^5L_6$ by Carnall and Fields[5] and is known to be strongly affected by the ligands[6]. It is seen from Fig.(9) and Table (10) that Am(III) species extracted by the tertiary amines should be distinctly different from that extracted by the quaternary amines. Whereas the aqueous phase absorption band for Am(III) occurs around 503 nm, that for Am(III) extracted by the tertiary amine is shifted bathochromically to about 510 nm and a considerable splitting is also observed. Comparatively, the shift obtained when quaternary amines are used as extractants for Am(III) is smaller. Moreover, there is a

Table - 10

Absorption Spectra of Am(III) extracted by long chain amine

Amine	λ_{max} (nm)	λ_{max}	Mean S.F. $K_d Am/K_d Eu$	Oscillator Strength
Tetraheptyl ammonium chloride 0.2M	503.4 509.3 515.5 522.0	261.3 38.2 - -	2.6	155.4×10^{-6}
Aliquat chloride 0.2M	504.0 509.6	95.7 47.8	4.7	85.9×10^{-6}
Aliquat chloride 0.1M	504.0 509.6	146.0 44.0	4.7	121.0×10^{-6}
Alamine-336 20%	509.6 512.7 521.2 523.0	38.0 (s) (s) 7.6	12.3	30.9×10^{-6}
Tri-iso-ootyl amine 20%	509.6 512.7 521.2	32.0 (s) (s)	63.2	26.0×10^{-6}
Tri-iso-ooty' amine 10%	509.6 512.7 521.2 523.0	36.0 (s) (s) 6.0	63.2	28.9×10^{-6}
Ethyl alcohol 7 M - HCl ($AmCl_6^{3-}$)	510 514 523	38 (s) 7	-	-
LiCl-KCl eutectic ($AmCl_x^{3-x}$)	506	160	-	-

x = 4,5

(s) represents shoulder only

marked lowering of absorption in the case of Am(III) extracted by tertiary amines which is strongly reflected in the oscillator strength values given in the last column of Table (10). Barbanel[7] and Marcus and Bomse[8] have shown from a study of Am(III) spectra in ethanolic HCl solutions that at 7 M HCl ("limit spectra") the species of Am(III) is $AmCl_6^{3-}$. The high (Oh) symmetry of the octahedral configuration makes the f-f transition spectacularly less allowed resulting in the overall lowering of absorption. Similarly Am(III) in CsCl-NaCl eutectic is also shown to be present as the species $AmCl_6^{3-}$. The closeness of the λ_{max} and ε_{max} values for Am(III) extracted by the tertiary amines indicates in agreement with Marcus[9] that the species extracted is $AmCl_6^{3-}$. The absorption spectra of Am(III) extracted by quaternary amines from LiCl in the present work is however markedly different but similar to those observed by Barbanel[7] for Am(III) in the LiCl-KCl eutectic wherein the presence of a four- or five- coordinated species of Am(III) namely $AmCl_{3+n}^{-n}$ (n = 1,2) was indicated. Existence of a lower chloro complex of Am(III) in the organic phase when quaternary amines are used as extractants can thus account for a lower degree of covalency in the Am(III) -chloride bonds which leads to a lower stability of the chloro complex, giving rise to lower separation factors.

REFERENCES

1. W.T. Carnall, P.R. Fields and B.G. Wybourne, J. Chem. Phys. 42, 3797 (1965).
2. J.L. Ryan, Inorg. Chem. 3, 211 (1964).
3. P.K. Khopkar and J.N. Mathur, J. Inorg. Nucl. Chem. 41, 391 (1979).
4. R.M. Diamond, K. Street and G.T. Seaborg, J. Am. Chem. Soc., 76, 1461 (1954).
5. W.T. Carnall and P.R. Fields, J. Chem. Phys. 40, 3428 (1964).
6. M. Shiloh, M. Givon and Y. Marcus, J. Inorg. Nucl. Chem., 31, 1807 (1969).
7. Yu.A. Barbanel, J. Inorg. Nucl. Chem p. 79, (Supplement 1976).
8. Y. Marcus and M. Bomse, Israel J. Chem., 8, 901 (1970)
9. Y. Marcus , Report 1A-1021, 35 (1965)

2.4.5 Recovery of Uranium and Plutonium from an Aqueous Solution Containing Phosphoric, Nitric and Sulphuric acids by Solvent Extraction

S.K. Patil, R. Thiagarajan and Rajendra Swarup

The most frequently used volumetric method[1] for the determination of uranium in nuclear fuel sample results in aqueous wastes containing phosphoric, sulphuric and nitric acids and appreciable quantities of uranium and plutonium. The present work was undertaken to develop a solvent extraction method for the separation of uranium and plutonium from such wastes.

Attempts to remove phosphoric acid selectively by multiple extractions with Amberlite LA-2 leaving U and Pu in the aqueous phase did not succeed. An alternate approach of extracting U and Pu directly from an aqueous phase containing phosphoric, sulphuric and nitric acids was pursued.

Preliminary experiments carried out with a number of extractants indicated that U(VI) and Pu(IV) could be quantitatively extracted by tri-n-octyl phosphine oxide (TOPO) in xylene. The distribution coefficient(K_d) data for U(VI) and Pu(IV) were obtained using 0.5M TOPO in xylene and various aqueous media (Table 11). The results showed that the extraction of U(VI) and Pu(IV) increased by addition of nitric acid or nitrate ions as reported in literature[2]. This suggested that the species of U(VI) or Pu(IV) extracted from an aqueous phase containing HNO_3, H_2SO_4 and H_3PO_4 were, predominantly the neutral nitrate complexes of U(VI) or Pu(IV) solvated by TOPO. This was confirmed by absorption spectral studies in the case of Pu(IV).

It was found that U(VI) could be quantitatively stripped from TOPO solutions with 0.5M ammonium carbonate. Back-extraction of Pu from TOPO solutions containing a few /ug/ml of Pu was studied using a number of stripping agents. The data show (Table 12) that Pu could only be stripped quantitatively with a mixture of HF and nitric acid. The presence of reducing agents favours the stripping. However, when experiments were carried out with macro-concentration of Pu(mg/ml), it was found that Pu was quantitatively back-extracted with ammonium carbonate solution. This behaviour was contrary to that observed earlier using lower concentration

Table - 11

Extraction of U(VI) and Pu(IV) by 0.5M TOPO in xylene

Aqueous phase	Distribution Coefficient (D) U(VI)	Pu(IV)
1M HNO_3	199	1493
1M H_2SO_4	9.8	6.3
1M H_3PO_4	0.083	0.25
1M H_2SO_4 + 1M H_3PO_4	1.6	1.7
1M H_2SO_4 + 1M H_3PO_4 + 1M HNO_3	56	371
1M H_2SO_4 + 1M H_3PO_4 + 2M HNO_3	49	-
1M H_2SO_4 + 1M H_3PO_4 + 4M HNO_3	34.4	-
1M H_2SO_4 + 1M H_3PO_4 + 0.5M NO_3^-	67.0	-
1M H_2SO_4 + 1M H_3PO_4 + 1.0M NO_3^-	63	-
1M H_2SO_4 + 1M H_3PO_4 + 2.0M NO_3^-	59	-
1M H_2SO_4 + 1M H_3PO_4 + 4.0M NO_3^-	59	-

NO_3^- ion concentration obtained using $NaNO_3$.

of Pu and was attributedto the change of oxidation state of Pu(IV) which resulted more rapidly at a higher concentration of Pu. This was confirmed by the absorption spectra of stripped Pu which showed a characteristic peak of Pu(III) at 600 nm.

The separation of U and Pu from the aqueous mixture by extracting into 0.5M TOPO followed by stripping with 0.5M ammonium carbonate

TABLE - 12

Back-Extraction of Plutonium from TOPO solution

Stripping Agents	Percentage of Pu stripped
0.5M $(NH_4)_2CO_3$	12
1M oxalic acid	35
0.2M HF	5
1MHF + 1MHNO_3	82
1MHF + 1MHNO_3 + 0.05M ferrous sulphamate + 0.05M NH_2OH HCL	89
2MHF + 1MHNO_3 + 0.05M ferrous-sulphamate + 0.05M NH_2OH HCL	97

was successfully tried with 100 mg of U and 10 mg of Pu. Uranium and plutonium from the back-extracted solution could be further purified by usual methods such as TBP extractions or anion-exchange after adjusting the acidity of the aqueous phase with nitric acid and oxidation state of Pu to Pu(IV).

References

1. W. Davies and W. Gray, Talanta, 11, 1203 (1964).

2. J. White and W. Ross, NAS-NS-3102 p. 44. (1961).

2.4.6 Complex Formation of Np(V)

S.K. Patil and N.M. Gudi*

In continuation of our studies on the complex formation of actinide ions with ligands in aqueous solutions by solvent extraction, studies were initiated on determination of stability constants at high ionic strength media. Very limited data on actinide complexes in such media have been reported. The complexing of Np(V) with various inorganic ligands, at an ionic strength of 8.5, was studied by solvent extraction method using sodium salt of dinonylnaphthalene sulphonic acid (NaDNNS) as the extractant. The results are summarized in Table 13.

TABLE - 13

Summary of the stability constants for Np(V) Complexes

μ = 8.5 pH ≃ 5 Temp = 25°C

Ligand	1	2	3
Cl^-	3.0	-	-
NO_3^-	0.26	0.43	-
SO_4^-	7.3	-	-
NO_2^-	2.2	11.7	-
SCN^-	8.2	11.7	53.5

* Fuel Reprocessing Division, B.A.R.C.

2.4.7 Anion-Exchange Studies of Neptunium in Mixed Solvent Media

S.K. Patil, M. Kusumkumari and Rajendra Swarup.

The work on the adsorption behaviour of neptunium on anion-exchange resin in mixed-solvent media was continued. The increase in the distribution coefficient (a) of Np(IV) on anion-exchange resin Dowex 1x4 (50-100 mesh) in the presence of methanol or acetone in 1M nitric acid indicated that the addition of methanol or acetone probably favours the formation of $Np(NO_3)_6^{2-}$ species. To substantiate this, adsorption spectra of Np(IV) in 1M HNO_3 and 1M HNO_3-90% methanol were recorded which showed a distinct absorption peak, around 877 nm, a characteristic of $Np(NO_3)_6^{2-}$ species, thus, supporting the inference. Based on the batch data of Np(IV) it was considered of interest to develop a method of separation of Np from other metal ions. The distribution coefficient data obtained for Pu(III), U(VI), Zr, Eu and Ru from 1M HNO_3-50% methanol revealed that a reasonably good separation of Np from these metal ions could be achieved.

Column experiments were carried out with a synthetic mixture of Np(IV) and Pu(III) from 1M HNO_3-50% methanol which gave 50% recovery of Np with a D.F. of 10,000 from Pu. Subsequently, the experiments with a mixture of Np(IV), Pu(III), U(VI) and Zr were carried out in a similar manner. Neptunium recovery was measured by α-counting of ^{239}Np and by estimating ^{237}Np spectrophotometrically as Arsenazo-III complex after masking Zr(IV), if any, with phosphoric acid. Results summarized in Table 14, show that though the recovery of neptunium was relatively low ($\sim$ 50%), the separation of Np from other metal ions was quite satisfactory.

TABLE 14

Summary of the results of the column experiments

Feed: ^{237}Np - 20 ug

Pu - 200 ug

U - 10 mg

Zr - 500 ug

in 10 ml of 1M HNO_3 - 50% methanol containing 0.05M ferrous sulphamate and $NH_2OH.HCL$.

No. of Runs	% Np recovery measured by α-counting of ^{239}Np	Spectrophotometry
1	40	42
2	42	45
3	41	41.3
4	40	38.5
5	48	50
6	37	41.3

2.5 Radiation Chemistry

2.5.1 Radiolytic Oxidation Mechanism of U(IV) to U(VI) in H_2SO_4 and HCl Media

P.K. Bhattacharyya and R.D. Saini

Considering the importance of U(IV) as a reductant for the separation of uranium and plutonium in the PUREX PROCESS, a systematic investigation on the radiation chemical behaviour of U(IV) has been undertaken[1,2] under various conditions. The results obtained are useful in proposing the mechanism for the oxidation without considering the earlier assumption involving chain reaction[3]. This report describes the work carried out on this topic during the period under report.

(A) In H_2SO_4 medium it is observed that values of $G(-U(VI)-)$ both in presence and absence of air are dependant on the concentration of U(VI). The limiting $G(-U(VI)-)$ values are shown in Table 15.

TABLE 15

$G(-U(VI)-)$ values under different conditions

Medium	$(-U(VI)-)$, mM	$G(-U(VI)-)_{air}$	$G(-U(VI)-)$
0.4M H_2SO_4	1	7.8	0.7
	5	8.5	1.2
	10	8.8	1.6
	25	9.0	-
	50	9.2	2
0.9M HCl	1	5.1	0.76
	2	6.5	1.0
	3	7.2	-
	4.4	7.7	1.15
	8.5	7.8	-
	10	-	1.3

The $G(U(VI))_{air}$ has a limiting value of ~ 9.2 in $0.4M H_2SO_4$ which can be explained by the following reaction mechanism.

$$H_2O \longrightarrow H, OH, H_2O_2, H_2 \quad (1)$$

$$H + O_2 \longrightarrow HO_2 \quad (2)$$

$$HO_2 + U^{4+} + H_2O \longrightarrow UO_2^{2+} + 2H^+ + OH \quad (3)$$

$$OH + U^{4+} + H_2O \longrightarrow UO_2^{+} + 3H^+ \quad (4)$$

$$2UO_2^{+} + 4H^+ \longrightarrow UO_2^{2+} + U^{4+} + 2H_2O \quad (5)$$

$$UO_2^{+} + OH + H^+ \longrightarrow UO_2^{2+} + H_2O \quad (6)$$

$$H_2O_2 + U^{4+} + H_2O \longrightarrow UO_2^{+} + OH + 3H^+ \quad (7)$$

From reactions (1) - (7)[4] one can evaluate $G(U(VI))_{air}$ 7.8 which is indeed the case at low concentration of U(IV). On the other hand, to explain the limiting $G(U(VI))_{air}$ 9.2 at the higher concentration of U(IV) (~ 50 mM) we consider that some aerial oxidation by the following reaction (8) is responsible.

$$UO_2^{+} + O_2 + H^+ \longrightarrow UO_2^{2+} + HO_2 \quad (8)$$

In deaerated H_2SO_4 media $G(U(VI))_{deaerated}$ values are explained on the basis of reactions (4) to (7) along with the folliwng reaction (9).

$$H + OH \longrightarrow H_2O \quad (9)$$

Thus, at high concentration of U(IV), reaction (4) predominantly explains the $G(U(VI))_{air}$ and $G(U(VI))_{deaerated}$ are significantly less than those in H_2SO_4 media (Table 15). This reduction of $G(U(VI))$ values are explained as due to the following reactions.

$$H^+ + Cl^- + OH \longrightarrow Cl + H_2O= \quad (10)$$

$$Cl + Cl^- \longrightarrow Cl_2^- \quad (11)$$

$$Cl_2^- + U^{4+} + 2H_2O \longrightarrow UO_2^{+} + 2Cl^- + 4H^+ \quad (12)$$

$$Cl_2^- + Cl_2^- \longrightarrow 2Cl^- + Cl_2 \quad (13)$$

$$Cl_2 + H \longrightarrow H^+ + 2Cl^- \quad (14)$$

Along with reactions (3) and (5) they explain the experimentally obtained $G(-U(VI)-)_{air}$ of 4.2 to 7.8.

References

1. P.K. Bhattacharyya and R.D. Saini, Ann. Prog. Report, Radiochem. Div. (1976) BARC Report-974 (1978).

2. P.K. Bhattacharyya and R.D. Saini, J. Inorg. Nucl. Chem. Letters, 13, 479 (1977).

3. M. Haissinsky and M. Duflo, J. Chim. Phys. 56, 955 (1959).

4. P.K. Bhattacharyya and R.D. Saini, (unpublished).

2.5.2 Flash Photolysis of Aqueous Potassium Persulphate Solution

P.K. Bhattacharyya and R.D. Saini

Flash photolysis of aqueous persulphate solution has been reported to give SO_4^- radical ion which is a very powerful oxidizing agent[1]. Thus it was thought that in the flash photolysis of aqueous persulphate solution containing Pu(VI), a reaction between Pu(VI) and SO_4^- radical should produce Pu(VII). However, before introducing Pu(VI) in the persulphate system it was necessary to investigate the spectral and kinetic behaviour of SO_4^- radical at different pH and in highly alkaline conditions wherein Pu(VII) has been reported to be fairly stable[2].

Flash photolysis of aqueous persulphate was carried out under various conditions in deaerated solutions. It was observed that although the absorption maximum of SO_4^- radical ion always occurred at 455 nm, its kinetics of decay changed from second order at lower pH to first order at high pH and under strongly alkaline conditions. The results are summarised in the Table 16.

The change in the order of kinetics can be explained by the following reaction

$$SO_4^- + H_2O \longrightarrow H^+ + SO_4^{2-} + OH \qquad (1)$$

Thus, at low pH due to an abundance of H^+ ion backward reaction predominates over the forward reaction thereby producing enough SO_4^- radical ions which predominantly combine to regenerate $S_2O_8^{2-}$ by a second order mechanism.

$$\text{i.e.} \quad SO_4^- + SO_4^- \longrightarrow S_2O_8^{2-} \qquad (2)$$

At high pH and under strongly alkaline conditions, on the other hand, the hydrolysis of SO_4^-, a pseudo first order process as indicated by the forward reaction of (1) is the main decay process of SO_4^- radical ion which leads to the observed first order kinetics.

In the absence of a reactive solute, OH radicals would generally combine to produce H_2O_2. Therefore, one of the end results of reaction (1) woule be the production of H^+ ion which should decrease the pH of

TABLE 16

Rate Constants for the Decay of SO_4^- at various pH

Sl.No.	System	Initial pH	After flash photolysis pH	λ_{max} nm	Rate constant k
1.	$K_2S_2O_8$(10 mM)+ H_2SO_4saturated with purified N_2	3.05	2.94	455	-
2.	-do-	4.62	3.74	455	$5.02 \times 10^8 M^{-1}S^{-1}$(2nd order)
3.	$K_2S_2O_8$(10 mM) saturated with purified N_2	6.57	3.74	455	$5.84 \times 10^8 M^{-1}S^{-1}$(2nd order)
4.	$K_2S_2O_8$(12.6 mM) + NaOH saturated with N_2	10.3	3.5	455	$4.7 \times 10^8 M^{-1}S^{-1}$ (2nd order)
5.	$K_2S_2O_8$ (10 mM) + NaOH saturated with N_2	12.4	12.4	455	$1.38 \times 10^3 S^{-1}$ (1st order)
6.	$K_2S_2O_8$ (10 mM) + NaOH saturated with N_2	1MNaOH	-	455	$5.4 \times 10^2 S^{-1}$ (1st order)
7.	$K_2S_2O_8$ (50 mM) + NaCl (1M) + KOH ($\sim$0.1M) saturated with N_2	12.3	12.3	455	$8.15 \times 10^2 S^{-1}$ (1st order)
8.	$K_2S_2O_8$ (50 mM) + NaOH + NaCl(1M) saturated with N_2	1MNaOH	-	455	$4.7 \times 10^2 S^{-1}$ (1st order)

the solution. The observed decrease in pH after flash photolysis, as can be seen from Table 16 supports reaction (1) (pH decrease ion measured after ~10-12 flashes).

References

1. E. Hayon et al. J. Phy. Chem. 71, 1472 (1967)

ibid 71, 2511 (1967)

ibid 71, 3802 (1967)

2. V.I. Spitsyn et al. J. Inorg. Nucl. Chem. 31, 2733 (1969).

2.5.3 LET and Cation Effects on the Radiolytic Formation of Nitrite in Solid Nitrates

P.K. Bhattacharyya and R.D. Saini

After establishing the mechanism for the formation of HNO_2 by gamma radiolysis of aqueous nitric acid solution[1], studies were initiated to investigate the effects of (i) the transition from solution to solid phase (ii) LET and of (iii) the nature of the cation on the formation of nitrite in the radiolysis of nitrates. Solids like KNO_3 and $UO_2(NO_3)_2.6H_2O$ crystals were irradiated in Co-60 gamma chamber and in the thermal column of Apsara reactor followed by the determination of the radiolytically produced nitrite. The results of some preliminary experiments are shown in Table 17 below :

TABLE 17

Radiolytic Yields of Nitrite

Sl. No.	Material Irradiated	Type of Radiation	$G(NO_2^-)$ ions/100 eV	Number of experiments
1.	KNO_3 crystals	^{60}Co -	0.98 ± 0.12	5
2.	$UO_2(NO_3)_2.6H_2O$ crystals	^{60}Co -	0.02	2
3.	-do-	Reactor Radiation in thermal column	2.69(a)	1
4.	-do-	Reactor Radiation in thermal column shielded by Cd foil	0.57(a)	1

(a) Excluding $G(NO_2^-)$ = 0.02 due to gamma-radiation.

It can be seen from these preliminary results that both LET and the nature of cation have a marked influence on the radiolytic yield of nitrite. The increase in $G(NO_2^-)$ with increasing LET may be due to the spin reactions of radicals like NO_3 and the formation of O_2 molecule with greater ease following reaction (1) due to radiation.

$$(NO_3^- \longrightarrow NO_3 + e^-)_{cage} \quad NO_3^- \qquad (1)$$

$$NO_3^- \longrightarrow NO_2^- + O \qquad (2)$$

$$O + O \longrightarrow O_2 \qquad (3)$$

The formation of O_2 molecule inhibits the recombination of NO_2^- and O to regenerate NO_3^-, thus resulting in a higher yield of NO_2^-. On the other hand, decrease in $G(NO_2^-)$ with the change of cation from K^+ to UO_2^{2+} may be due tothe redox reactions of the latter with radiolytically produced NO_2^-. However, further experiments are necessary to understand in detail the mechanism of the radiolytic formation of NO_2^- in such solids.

References:

1. P.K. Bhattacharyya and R.D. Saini, Int. J. Radiat. Phy. Chem. 5, 91-99 (1973).

Section: 3 - PROCESS CHEMISTRY

3.1 Preparation of Plutonium - 238

C.K. Sivaramakrishnan, A.V. Jadhav, K. Raghuraman, K.A. Mathews and P.S. Nair.

Five one gm samples of ^{237}Np as NpO_2 were wrapped in aluminium foils and sealed in CIRUS cans. Details of irradiation and handling of the samples described in the annual report 1977[1]. All the five targets along with their aluminium foil wrappers were dissolved in 7M HNO_3. After ensuring complete dissolution an aliquot of the solution was taken to assay total ^{238}Pu present. This assay showed the total ^{238}Pu in the solution to be 175 mgs. Oxidation state of plutonium and neptunium were adjusted to 4 by addition of excess of ferrous sulfamate and heating the solution for one hour at 55°C. Pu(IV) and Np(IV) were then co-absorbed on 4Cm × 20Cm Dowex-1 (50-100 mesh) anion exchange column. The column was thoroughly washed to remove the bulk of the fission products. Plutonium and neptunium were then coeluted with 0.35 M HNO_3. This step provided enough decontamination from fission products to permit transfer for subsequent purification in a glove box of ^{238}Pu from neptunium.

Reference

1. Radiochemistry Division Annual Progress Report for 1977 - BARC-1005(1979) 12.

3.2 Process Chemistry of Neptunium

S.V. Kumar*, M.N. Nadkarni*, P.K.S. Kartha*, N.M. Gudi* and S.K.Patil

In continuation of our studies onthe process chemistry of neptunium, work was initiated to explore the use of primary or secondary amines for the purification and concentration of neptunium. The batch data for the extraction of Np(IV), Np(VI), Pu(III), Pu(IV) were obtained using 20% Primene JMT and 20% Amberlite LA-1 dissolved in solvesso-100 at varying concentration of nitric acid. These are summarised in Table 18. The data show that extraction of both Np(IV) and Pu(IV) is

---

* Fuel Reprocessing Division.

TABLE 18

Distribution Coefficient Data of Np(IV), Np(VI), Pu(III), Pu(III) and U(VI) from nitric acid medium using Primary and Secondary amines as the extractants

$[HNO_3]$ M	20% Primene JMT in Solvesso-100			20% Amberlite LA-1 in Solvesso.100				
	Np(IV)	Np(VI)	Pu(IV)	Np(IV)	Np(VI)	Pu(IV)	Pu(III)	U(VI)
0.5	-	-	-	0.055	0.1	-	$9x10^{-4}$	-
1.0	0.0008	$8x10^{-4}$	-	0.33	0.26	2.5	$7x10^{-4}$	0.07
1.5	-	-	-	-	-	-	$15x10^{-4}$	-
2.0	0.002	$cx10^{-3}$	0.009	1.16	0.63	5.4	$14x10^{-4}$	0.14
2.5	-	-	-	-	-	-	$12x10^{-4}$	-
3.0	0.009	-	-	1.86	-	-	$15x10^{-4}$	-
4	0.034	0.07	0.13	2.59	1.4	11.2	-	0.32
5	0.11	-	-	3.47	-	-	-	-
6	0.31	0.03	0.96	4.57	-	16	-	0.52
7	0.73	-	-	5.4	-	-	-	-
8	1.38	0.131	2.6	5.7	-	14	-	0.53

more with LA-1 than that obtained under similar conditions with Primene JMT. The extraction of Pu(III) into LA-1 is much less than that of Np(IV) under the same conditions and this suggests that good separation of Np(IV) from Pu(III) could be obtained by LA-1 extraction. The separation of Np(IV) from U(VI) however may not be very good.

3.3 Some Studies on the Extraction of Rare Earths by TBP

S.M. Jogdeo*, Madan Pal*, S.K. Patil, S.P. Gandhe and R. Thiagarajan

The extraction behaviour of rare earths under the conditions relevent to uranium refining by TBP was investigated. The distribution coefficient data for the extraction of Gd were obtained at varying concentrations of nitric acid and TBP. Typical data, summarized in Table 19; show that when the uranium loading of TBP is ~100 g/l, Gd is practically inextractable into TBP. Counter

TABLE 19

Variation of Distribution Coefficient (Kd) of Gd with Uranium Loading Initial aqueous acidity=3M

Initial $(U)_{aq}$ mg/ml	Eq. U Concentration.mg/ml		Kd (Gd)
	Org	Aq	
-	-	-	0.07
3.51	2.99	0.50	0.07
17.54	15.56	2.34	0.05
70.15	55.66	12.27	0.01
105.22	74.81	24.54	0.003
140.29	93.36	40.1	0.0007
210.24	113.71	82.59	-
280.58	126.88	140.04	-
350.73	134.06	196.3	-

* Uranium Metal Plant.

current extraction experiments were carried out to study the extraction of Tb under conditions used in uranium refining process. The results of a typical experiment are summarized in Table 20.

TABLE 20

Counter Current Extraction Behaviour of Tb

Feed: $[U]$ = 200 g/l; $[HNO_3]$ = 3M; $[Tb]$ = 1.7×10^5 cpm/ml;
Flow rates (ml/min) : Feed = 2.75; or g = 5.6;
Residence time/stage = 1 min.

Extractant: 33% TBP in SST

Time Hrs.	^{160}Tb activity in outgoing streams cpm/ml x 10^{-3}		U loading g/l
	Aqueous	Organic	
15.40	188	0.22	110
16.40	188	0.26	108
17.40	187	0.31	107
18.40	178	0.72	98
19.40	186	0.40	107
Avg.	186	0.38	106

D.F. = 230

From the Tb activity following uranium in the organic stream, it was concluded that excellent decontamination of U from Tb was achieved (DF 230) where uranium loading of the organic phase was $\sim$105 g/l.

Experiments were carried out to study the kinetics of forward and reverse extraction of Tb by TBP using AKUFVE set up. The data revealed that with Tb activity present, initially either in the aqueous or the organic phase, the equilibrium is reached in a few seconds.

3.4 In-line Analysis of Fuel Reprocessing Streams

V.K. Rao, S.G. Marathe, V.K. Bhargava and R.H. Iyer.

Most of the effort was put in 'in-line' testing and the reliability in performance and stability of gamma absorptiometer and colorimeter at Fuel Reprocessing Division*. About 150 samples were analysed by using gamma absorptiometer and results were compared with laboratory analyses. These results were obtained by correcting for the zero shift are not in accordance with any continuous 'in-line' monitoring instruments the unit was found to have a definite zero drift during a prolonged period, efforts were made to eliminate the drift by improving the electronics associated with the gamma absorptiometer. After making necessary requirements the unit seems to work satisfactorily.

In the case of colorimeter, problems were encountered due to vibrations, turbidity and flow rate. Some changes like providing padding for lamp house and photo cell compartment are contemplated to eliminate the drift due to vibrations.

---

* In collaboration with Shri S.V. Kumar.

SECTION 4: RADIOANALYTICAL CHEMISTRY AND SERVICES

4.1 Determination of Isotopic Composition of Plutonium using Gamma Ray Spectrometry

S.B. Manohar, S.K. Agarwal, S.M. Deshmukh, P.P. Burte, A.R.Parab, H.C. Jain, Satya Prakash and M.V. Ramaniah.

The gamma spectrometric method for the determination of isotopic composition of plutonium offers some distinct advantages. This method is non-destructive, comparatively fast with possible adaptability to a wide variety of configurations as well as can be used for unambigeous identification of plutonium lots. However, the method depends on calibration based on the more accurate mass spectrometric method.

In the present work, an attempt has been made to develop the method covering relatively a wide range of burn up (Table 21) than

TABLE 21

The range of isotopic composition used for calibration purpose *

Isotope of plutonium	Range in Atom %
^{238}Pu	0.01 to 0.80
^{239}Pu	95 to 63
^{240}Pu	5 to 26
^{241}Pu	0.3 to 7.5

* This range covers the isotopic composition of plutonium obtained from reprocessing of LWR fuel with burn up in the range of 2000 to 20,000 MWD/T.

hither-to reported in earlier investigations. The plutonium required for this purpose was obtained by ion exchange purification of small samples of irradiated fuel pins of different burn up cut at various positions along the length of the fuel pin to provide a range of burn up. Fifteen such samples were prepared and purified free of

fission products and ^{241}Am and assayed gamma spectrometrically and mass spectrometrically. Working curves of atom present Vs gamma ray activity ratio for different isotopes of plutonium have been thus constructed using gamma rays in 40 to 150 KeV energy zone. In the present determinations samples of 200 to 500/ug of plutonium were counted which gives accuracies for different isotopes in the range of 1 to 5%. However, a shorter counting duration and better accuracies (~1%) can be achieved if larger sample sizes (10-50 mg of plutonium) are counted. A typical set of results are given in table 22.

TABLE 22

Sample No.	The isotopic composition of the Pu sample Gamma Spectrometry				Mass Spectrometry			
Isotope	238	239	240	241	238	239	240	241
G - 12	0.0773	88.43	9.415	1.454	.08225	88.22	9.1957	1.465
G - 14	0.889	70.16	21.64	6.707	.855	68.36	21.500	6.966

A few experiments have been conducted to establish the intrinsic nature of the technique and it is found that the change in counting geometry do not affect the results of ^{238}Pu, ^{239}Pu and ^{240}Pu. Further work is in progress to check in detail the effects of geometry on accuracy with higher amounts of plutonium.

References:

1. Gunnink, R., and Morrow, R. UCRL - 51087 (1971).

2. Gibbs, A. DPSPU - 74-11-20 (1974)

3. Umezawa, U., Suzulei, T. and I Chilcawa, S., J. Nucl. Sci. Tech. 13, 327 (1976).

4.3. Precision and Accuracy in the Determination of $^{238}Pu/(^{239}Pu + ^{240}Pu)$ Alpha Activity Ratio by Alpha Spectrometry

S.K. Aggarwal, S.A. Chitambar, V.D. Kavimandan, A.I.Almoula, P.M. Shah, V.L. Sant, A.R. Parab, H.C. Jain and M.V.Ramaniah

With a view to utilising ^{238}Pu as a spike and using the principle of isotope dilution for determining the concentration of plutonium in irradiated fuel dissolver solutions, it was considered essential to evaluate the precision and accuracy in the determination of $^{238}Pu/(^{239}Pu + ^{240}Pu)$ alpha activity ratio by alpha spectrometry. Further the objective was to evolve a simple evaluation procedure for computing the alpha activity ratios which could be routinely used without resorting to complicated computer programmes. The alpha activity ratios considered were in the range of 0.01 to 10 so that isotope dilution alpha spectrometry (IDAS) could be employed for the precise and accurate determination of plutonium in various dissolver solutions from fuel having different burn-up values.

For this purpose, different synthetic mixtures with alpha activity ratios ranging from 0.01 to 10 were prepared using enriched isotpes of ^{238}Pu and ^{239}Pu. The solutions of ^{238}Pu and ^{239}Pu were purified from ^{241}Am using ion exchange procedure. The radiochemical purity of the purified solutions was checked by alpha spectrometry and gamma spectrometry. The master solutions of ^{238}Pu and ^{239}Pu were assayed by liquid scintillation counting for the determination of alpha disintegration rate. Thirteen synthetic mixtures with $^{238}Pu/(^{239}Pu + ^{240}Pu)$ alpha activity ratios ranging from 0.01 to 10 were prepared by mixing the pre-calculated and accurately weighed aliquots from the master solutions. The alpha activity ratios of these mixtures were calculated by using the alpha disintegration rate of the master solutions and the aliquot weights.

For alpha spectrometry, electropolished stainless steel planchets were used as the backing material and the sources were prepared by electrodeposition in the aqueous nitric acid medium. Three electrodeposited sources were prepared from each of the synthetic mixtures.

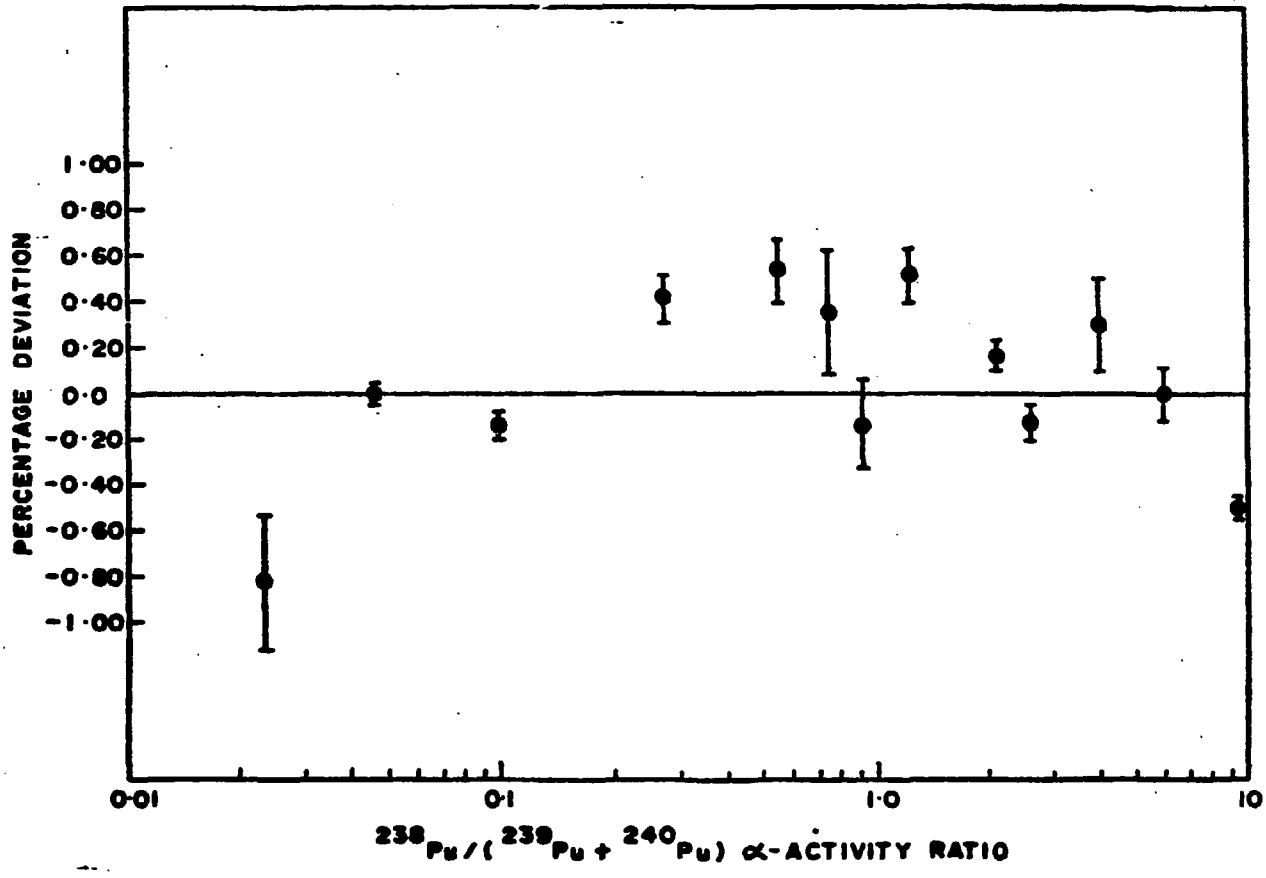

FIG.- 10.

Precision And Accuracy in the Determination of ^{238}Pu / (^{239}Pu + ^{240}Pu) - Activity Ratio

(From Electrodeposited Sources)

The alpha spectra from the sources were recorded by using a 50 mm^2 silicon surface barrier detector mounted in a vacuum chamber and coupled to a 4k analyser (TN-1700). The system has a resolution of 20 KeV (FWHM) at 5.50 MeV. The alpha spectrum from each of the electrodeposited sources was recorded thrice. The sources were counted for a time long enough to accumulate more than 10^5 counts in each of the two peaks.

The alpha activity ratios from the alpha spectra were computed by three different methods. In the first method, the alpha activity ratio was computed by taking the pre-selected channel regions (equal number of channels) for ^{238}Pu and (^{239}Pu + ^{240}Pu) peaks and no correction was applied for the contribution of high energy peak to the low energy peak. In the second method, the correction due to energy degradation was applied based on the contribution in (^{239}Pu + ^{240}Pu) peak region as observed from the pure ^{238}Pu source. If R_0 is the observed alpha activity ratio obtained by first method and R_p is the activity ratio in the corresponding regions from the alpha spectrum of pure ^{238}Pu sources then corrected alpha ratio

$$R_c = \frac{R_o}{1 - R_o/R_p}$$

In the third method, the alpha activity ratio was computed by making different assumptions about the nature of energy degradation namely geometric progression (G.P.) decrease and linear decrease[1]. The results obtained by using these different evaluation methods are given in Table 23.

From the results given in Table 23, it is obvious that the first method should not be used for evaluating the alpha spectrum as it does not take into account the energy degradation correction. The second method which involves the correction due to energy degradation based on the alpha spectra from pure ^{238}Pu may be employed so long as the activity ratio is low. Further, the correction factor should be established for the alpha spectrometric set up being used and the pre-determined channel regions used for taking peak areas. The third group of methods based on decrease in G.P. and linear decrease lead to an accuracy of 0.5% or better in the range of alpha

activity ratio from 0.01 to 10. A graphical representation of the precision and accuracy achievable in alpha spectrometry is given in Figure (10). It is proposed to exploit alpha spectrometry for the concentration measurement of plutonium in the irradiated fuel dissolver solution by employing ^{238}Pu as a spike

TABLE 23

Comparison of different evaluation methods used for the computation of $^{238}Pu/(^{239}Pu + ^{240}Pu)$ alpha activity ratio from the alpha spectrum from electrodeposited source

Sl. No.	Synthetic mixture code No.	True value of $^{238}Pu/(^{239}Pu+^{240}Pu)$ activity ratio	Value computed from the alpha spectrum			
			I Method	II Method	III Method	
					G.P.	Linear
1.	SM-89-24	0.023584	0.023540	0.023544	0.023532	0.023531
2.	SM-89-25	0.04632	0.04623	0.04624	0.04621	0.04621
3.	SM-89-26	0.10121	0.10122	0.10130	0.10128	0.10128
4.	SM-89-13	0.27322	0.27372	0.27433	0.27430	0.27430
5.	SM-89-14	0.54874	0.55092	0.55340	0.55330	0.55328
6.	SM-89-15	0.74533	0.73742	0.74187	0.74151	0.74148
7.	SM-89-16	0.9207	0.9082	0.9149	0.9196	0.9192
8.	SM-89-17	1.2305	1.2361	1.2384	1.2382	1.2380
9.	SM-89-18	2.0395	2.0107	2.0441	2.0422	2.0414
10.	SM-89-19	2.5269	2.4870	2.5383	2.5300	2.5293
11.	SM-89-30	4.0097	3.8934	4.0207	4.0027	4.0001
12.	SM-89-32	6.3339	6.0999	6.4182	6.3573	6.3515
13.	SM-89-33	9.6063	8.9976	9.7077	9.5697	9.5552

and using the principle of isotope dilution. Work in this connection has already been initiated and the results are quite encouraging.

References

1. Shunji Umemoto, Radiochimica Acta, 8, 107 (1967).

4.4 Feasibility of Isotopic Abundance Measurement of Uranium at Nanogram Level using thermal Ionization Mass Spectrometry

V.D. Kavimandan, S.S. Desai*, S.A. Chitambar, S.N. Acharya, S.R. Desai, J.P. Mittal** and H.C. Jain

A number of samples (~10 ng of uranium) collected on the surface of a target are expected to be generated for isotopic abundance measurement from laser experiments. Thus it was considered essential to find a suitable target material free from uranium and easy to process chemically for recovering uranium from bulk of target material without picking up of any uranium at any step. A number of experiments were conducted to find out the uranium blank from superpure target materials like aluminium, tantalum and silver foils. The uranium content was determined by isotope dilution mass spectrometry using 10 ng of enriched ^{235}U as spike. The neutron activation analysis of the aluminium foil confirmed that the uranium in the blank is coming from the target material rather than as pick up in chemical processing. Two different lots of super pure aluminium foil and tantalum foil were tried but the uranium content was found to be 100-200 ppb while silver foil was found to be much superior and the blank was only 5 ppb.

Finally silver foil has been found to be suitable as it contains much less amount of uranium, only part of the foil need be dissolved for stripping collected uranium and the chemical separation of uranium from bulk of silver is simple and quick. The neccssary experience has been gained in working with about 10 ng level of uranium on about 20 samples without picking up any uranium by observing the necessary precautions like distilled reagents, and leached glass wares and cleanliness of the working place.

---

* Analytical Chemistry Division, BARC.

** Chemistry Division, BARC.

4.5 Maintaining High Abundance Sensitivity Improvement and Monitoring of Vacuum of Analyser and Collector Regions of the CH-5 Mass Spectrometer

C.S. Subbanna*, P.S. Srinivasan and U.C. Jain

It order to maintain high abundance sensitivity, it was considered essential to improve the vacuum at the analyser and collector region of the CH-5 mass spectrometer. A Vac-Ion pump along with its fittings which could be directly connected to the instrument was costing more than Rs.50,000/- when obtained from the supplier of the Mass spectrometer while the cost of a Vac-Ion pump was only Rs.10,000/-. Thus it was decided to buy a Vac-Ion pump and make the necessary flanges and fittings at the divisional workshop.

Two flanges were designed, fabricated and Argon arc welded to the two ports of Philips Granville Ultra-High-Vacuum valve. This was leak tested using a helium leak detector. Leak tightness was found to be better than 10^{-10} std cc/sec. Design of connecting flanges was such that one side could be connected to the mating flange on the collector side of the mass spectrometer and the other side to the mating flange on Vac-Ion-Pump. Suitable fixtures were used to mount the Vac-Ion-Pump on the mass spectrometer rack. Electronic control units of the pump were suitably accommodated in the Electronics-console-rack of the mass spectrometer.

After installation of the Vac-Ion-Pump, pressure in the analyserregion of the mass spectrometer during routine analysis is now less than 10^{-7} torr and abundance sensitivity greater than 10^{-5} is observed as a routine feature compared to frequent fluctuations before Vac-Ion-Pump was mounted.

---

* Staff of NUMAC.

4.6 Development of a Method for the preparation of High Superficial Density Fissile Sources

V.S. Mallapurkar, R.J. Singh, A.V.R. Reddy, C.R. Venkatasubramani, S.S. Rattan, and Satya Prakash

Sources of 100-200 /ug/cm^2 superficial density of actinide isotopes can be prepared by electrodeposition from non-aqueous media like alcohols and of somewhat lower amounts from aqueous media. Higher depositions result in the formation of deposits with very poor adherence. Attempts have been made to achieve the higher depositions using electrophoretic methods of deposition on silver backings and finally covering the deposits with silver itself for safe handling before and after irradiation.

The method, in brief, consits of taking the oxide of the material deposited (UO_2 in the present work) and grinding the oxide to fine grains by means of a pestle and morter. A suitable amount of ground oxide is taken in about 100 ml of isopropyl alcohol and put in an ultrasonic generator for about 15-20 minutes. This results in the suspension of finer grains in the alcohol. The material is left for a few hours undisturbed and the suspension thus obtained was used for electrophoretic deposition. About 10 ml of the suspended oxide is taken in the deposition cell. The silver plancette forms the cathode and a platinum wire acts as anode. A deposition voltage of about 1000 volts is applied for the electrophoretic migration. The suspended grains of oxide migrate to deposit on silver cathode. In about two hours almost quantitative deposits have been obtained. Deposits with a maximum surface density of 20 mg/cm^2 have been made.

These targets are covered by silver from the top by vacuum evaporation of silver. In another method target is covered by another silver foil joining the two foils by silver alloy brazing foils.

Further work to study, in greater detail, the particle size suspension, the deposition rates, best choice of suspension media etc. is in progress. Targets thus prepared are also going to be subjected for irradiation.

4.7 Potentiometric Estimation of Neptunium

S.K. Patil and A.G. Godbole

The work on the development of potentiometric methods for the determination of neptunium by redox titrations was continued. It is known that in dilute perchloric acid media Fe(II) reduces Np(VI) to Np(V) quantitatively and Np(V) thus formed is not reduced significantly to Np(IV) by Fe(II). Experiments carried out at varying concentrations of perchloric acid showed that in 0.3M $HClO_4$ medium, reduction of Np(V) to Np(IV) by Fe(II) is negligible. A potentiometric method was developed based on these data. The method consists of oxidation of Np(IV) to Np(V) by addition of excess ferrous perchlorate in 0.3M perchloric acid medium and subsequently titrating the excess Fe(II) potentiometrically with Ce(IV). The precision of the method was better than ± 1% for aliquots containing 3-8 mg of neptunium. The results obtained by this method were in good agreement (within ± 1%) with the values obtained by coulometry and potentiometry[1].

4.8 Determination of Boron in Boron Carbide

V.K. Manchanda and M.S. Subramanian

Boron carbide is an important nuclear material as it used in nuclear reactors for control rods and as a shielding material. The main impurities in boron carbide are unreacted carbon or boric acid, which affect the physical, chemical and neutron absorption properties of the material. Thus it is of interest to develop analytical procedures for the precise determination of various constituents in boron carbide.

In this context, a volumetric method for the estimation of boron in boron carbide has been perfected. The method involves fusing the sample with fission mixture and titration of boric acid in the presence of hydrochloric acid using p-nitrophenol (pK_a = 7.1) and phenolphthalein as indicators. Repeated analysis of a sample of boron carbide by this procedure gave a standard deviation of ± 1.2% (Table 24).

---

1. A.G. Godbole and S.K. Patil Talanta (In press).

TABLE 24

Analysis of a Boron Carbide Sample

S.No.	Weight of the sample(mg)	% of Boron
1.	24.075	74.95
2.	21.490	75.76
3.	20.680	75.84
4.	26.430	75.97
5.	20.725	73.94
6.	22.527	75.81
7.	11.395	77.72
8.	17.146	75.13
9.	19.930	75.27
10.	22.560	75.70
11.	13.525	76.14
12.	16.037	75.84

Average % Boron = 75.67

Standard Deviation(σ) = 0.9

r.S.D. = $\pm$ 1.20%

4.9 Extractive-photometric Determination of Neptunium (IV) and Plutonium (IV) when present together

J.P. Shukla and M.S. Subramanian

Following the development of an extractive-photometric method for the determination of trace amounts of neptunium and plutonium from their mixtures is described. Neptunium is selectively extracted from about 1M HNO_3 with TTA in xylene retaining Pu in the non-extractable trivalent state in the aqueous phase with ferrous sulphamate. The neptunium thus extracted is determined at 535 nm after developing the colour with xylenol orange.

TABLE 25

Analysis of Np and Pu from their mixtures

Taken, µg		Found*, µg		Error, %	
Np^{4+}	Pu^{4+}	Np^{4+}	Pu^{4+}	Np	Pu
0.85	1.00	0.87	1.02	2.35	2.00
1.37	1.66	1.42	1.63	2.16	1.81
2.06	2.60	2.03	2.55	1.46	1.92
2.41	3.01	2.36	3.07	2.07	1.99

* Average of 3 determinations of the sample

Plutonium in the aqueous phase is subsequently oxidised with $NaNO_2$ to the tetravalent state and extracted with TTA and estimated at 540 nm after development of colour with xylenol orange. Their molar absorptivities are in the 5×10^4 range. Beer's law has been found to be valid upto 2.4 ppm Np and 3.5 ppm Pu. The colour of the solution has been found to be stable for at least 48 hours. The method tolerates large excesses of several common contaminants encountered during spent fuel reprocessing. Cerium (IV) and phosphoric acid, however interfere, with the final estimation. Table 25 summarises, the results of analyses of representative samples of neptunium and plutonium when present together.

4.10 Mass-Spectrometric Services

S.A. Chitambar, V.D. Kavimandan, S.K. Aggarwal, R. Bagyalakshmi, K.L. Ramakumar, C.S. Subbanna*, A.I. Almoula, P.M. Shah, P.A. Ramasubramanian, S.N. Acharya, P.S. Khodade, V.A. Raman, V.L. Sant, A.R. Parab, H.C. Jain and C.K. Mathews.

The mass spectrometry section continued to provide mass spectrometric analytical services to various divisions of this establishment and DAE. During the year under report, more than 1200 mass spectrometric determinations were carried out. This includes about 400 samples of various elements received from different divisions of BARC

* Staff of NUMAC

and other units of DAE and the remaining were generated from the R & D activities of this Division.

In continuation of the Audit analysis of uranium and plutonium at PREFRE, Tarapur, mass spectrometric determinations were carried out on 12 input batches of irradiated fuel dissolver solution. 37 finished product uranium samples were analysed for plutonium present at ppm level by isotope dilution mass spectrometry(IDMS). Radiometric assay of plutonium was also carried out on more than 80 samples from the tank containing radioactive waste for disposal.

4.11 Supply of Special Radioactive Sources

Kum. V. Mallapurkar, R.J. Singh, and Satya Prakash

Fifty two electrodeposited sources of a number of actinide isotopes from ^{232}Th to ^{252}Cf were supplied to different users in BARC, other units of DAE and otheruniversities in the country. These sources were prepared meeting requirements of shape, size and level of activity tailored to users need.

4.12 Preparation of Radiation Sources

C.K. Sivaramakrishnan, A.V. Jadhav, K. Raghuraman, K.A. Mathews and P.S. Nair.

One 15 mci and 10 mg ^{241}Am radiation source for use as excitation source for X-ray fluorescence analysis, was fabricated and supplied to the user division of this research centre.

SECTION 5: NUCLEAR CHEMISTRY

5.1 Fission Studies

5.1.1 Charge Distribution in Low Energy Fission

Investigations on the influence of fragment shells and excitation energy on width of the charge distribution in low energy fission was undertaken for $^{245}Cm(n_{th},f)$ and $^{237}Np(n,f)$. A brief description of the work carried out is given below.

5.1.1.1 Determination of Fractional Cumulative Yields of ^{140}Ba and ^{95}Zr in the Thermal Neutron Induced Fission of ^{245}Cm

T. Datta, S.P. Dange, S.B. Manohar, A.G.C. Nair, Satya Prakash and N.V. Ramaniah.

Electrodeposited targets of ^{245}Cm ($\sim$ 3 μgm) covered with 1 mil thick aluminium catcher foils were irradiated in the reactor APSARA at neutron flux$\sim 10^{12}$ n/cm^2/sec and CIRUS at neutron flux $\sim 10^{13}$n/cm^2/sec. The irradiation time was varied from 90 minutes to 6 hours.

After appropriate cooling the aluminium catcher foils were mounted in a standard geometry and counted on a 60 cc Ge(Li) detector coupled to a 4096 channel analyser. The resolution of the detector was 1.5 KeV at 122 KeV and 3.9 KeV at 1332 KeV. Direct gamma counting of 487 KeV and 1596 KeV gamma peaks of ^{140}La and 765 KeV gamma peak of ^{95g}Nb were carried out for suitable period.

The isobaric chains studied are

$$^{95}Y \xrightarrow{\beta^-} {}^{95}Zr \xrightarrow{\beta^-} {}^{95g}Nb \xrightarrow{\beta^-} {}^{95}Mo$$

103 m 64.0 d 35.15 d Stable

$$^{140}Cs \xrightarrow[\beta^-]{} {}^{140}Ba \xrightarrow[\beta^-]{} {}^{140}La \xrightarrow[\beta^-]{} {}^{140}Ce$$

64 s 12.8 d 40.2 h Stable

Since the precursors of ^{95}Zr and ^{140}Ba are short lived compared to the time of irradiation and interval between the end of irradiation

and start of counting, the mass chains 95 and 140 were assumed to consist of ^{95}Zr - ^{95g}Nb and ^{140}Ba - ^{140}La respectively. Thus following the growth and decay of the daughter products ^{95g}Nb and ^{140}La, the fractional cumulative yields of ^{95}Zr and ^{140}Ba were obtained using the equations

$$Y = K N_1^{\circ} X + K N_2^{\circ} \qquad (1)$$

where

$$Y = \frac{A.t'}{t''} \cdot \frac{\lambda_2 \, e^{\lambda_2 T}}{(1-e^{-\lambda_2 t})\,(1-e^{-\lambda_2 t'})} \times \left(\frac{1-e^{-\lambda_1 t'}}{1-e^{-\lambda_2 t'}}\right) \qquad (2)$$

$$X = \left[1 - \frac{\lambda_2}{\lambda_2-\lambda_1}\left\{1 - \left(\frac{\lambda_2}{\lambda_1}\right)\left(\frac{1-e^{-\lambda_1 t}}{1-e^{-\lambda_2 t}}\right)\right\} e^{(\lambda_2-\lambda_1)T}\right] \qquad (3)$$

where K is a constant inclusive of rate of fission, detector efficiency etc.

A_2 is observed area of the photopeak of interest, t is the irradiation time, T is interval between end of irradiation and start of counting time. t' is the live time, t'' is clock time.

λ_1 & λ_2 are decayconstants of parent and daughter respectively. N_1° is the number of atoms of parent formed at the end of irradiation. N_2° is the number of atoms of daughter formed independently at the end of irradiation.

From the least square fitted plot of Y vs X the slope and intercept were obtained wherefrom

$$FCY = \frac{N_2^{\circ}}{N_1^{\circ} + N_2^{\circ}} = \frac{\text{slope}}{\text{slope + intercept}}$$

Results

The FCY values are given in Table 36. The value for ^{140}Ba shows a broader width parameter for the assumed gaussian charge distribution compared to usually observed width value of 0.56 ± 0.006.

TABLE 26

Fissioning nucleus	Fission product	FCY value
$^{245}Cm + n$	^{95}Zr	0.957 ± 0.001
	^{140}Ba	0.969 ± 0.006

5.1.1.2 Determination of Fractional Cumulative Yields of ^{135}I and ^{140}Ba in Reactor Neutron Induced Fission of ^{237}Np

S.B. Manohar, P.P. Burte, S.M. Deshmukh, Satya Prakash and M.V. Ramaniah.

Charge distribution studiesin the fission of ^{237}Np have been initiated since there is no data on charge distribution for an odd fissioning nucleus, so as to understand the odd-even effect in terms of Z of the fissioning nucleus. The work on two mass chains have been started with reactor neutron.induced fission.

The isobaric chain of mass number 135 studied is

$$^{135}Te \xrightarrow[18\ s]{\beta^-} {}^{135}I \xrightarrow[6.59\ h]{\beta^-} {}^{135}Xe \xrightarrow[9.59\ h]{}$$

While the isobaric chain of mass number 140 is given in 1.1.1. The experimental procedure used and equations are similar to that described in sec. 1.1.1. In order to abhieve the highest flux of higher energy the irradiations were carried out in Apsara reactor and the target was wrapped with Cd foil (1 mm). The value of 0.945 ± 0.01 was obtained for ^{135}I and a tentative value of ^{140}Ba has been obtained. Further work is in progress on ^{140}Ba and other mass chains.

5.1.2 Determination of the Average Angular Momentum of Fission Fragments in Low Energy Fission

The studies on independent formation of fission fragments with large angular momenta from compound nucleous of low initial angular momentum is a field of great interest. The angular momentum distribution of primary fission fragments has been of great importance

because it provides the information about the properties of the fissioning nucleus between saddle and the state shortly after scission configuration. The large angular momenta of fission fragments have been interpreted in terms of the excitation of the rotational levels of the deformed fragments which interact in the strong coulomb field for non-linear scission configuration.

The work on the radiochemical determination of the independent yield ratio (m/g) at different fission products has been undertaken with the aim to find out the average angular momentum of fission fragments and their correlation to Z and A of the fissioning system, their excitation and kinetic energy and fragment deformations.

The angular momentum of the fission fragments can be estimated from the measurements on number of prompt gamma rays together with its anisotropy or from the intensities of gamma transition in the rotational levels of even products as well as from the measurement of indepenent yield ratios of fission product isomers of known spins, radiochemically.

5.1.2.1 Determination of the Average Angular Momentum of Fission Product ^{132}I in $^{233}U(n_{th},f)$.

T. Datta, S.P. Dange, A.G.C. Nair, Satya Prakash and M.V. Ramaniah

The average angular momentum of fragments corresponding to fission product isomers ^{132m}I and ^{132g}I has been determined radiochemically and subsequently a calculation of fragment angular momenta as a function of various even-even mass splits has been carried out in order to see the correlation between fragment angular momentum and deformation.

Electrodeposited target ($\sim$600 /ugm) of ^{233}U was irradiated for 15 minutes in APSARA reactor in flux$\sim 10^{12}$ n/cm^2/sec. Fission products were collected in aluminium catcher foils and after irradiation, iodine was seperated radiochemically using appropriate dissolution and purification procedures. The sample was counted for the 772 KeV gamma peak of ^{132}I on a 60 cc.Ge(Li) detector

connected to a 4096 channel analyser in five time and for suitable duration over 6 to 7 hours. The peak area of the 772 KeV peak of abundance 76.2% from ^{132g}I and 13.2% from ^{132m}I was related to the independent yields Y_m^i for ^{132m}I and Y_g^i for ^{132g}I using the relation

$$Y = R. Y_m^i X + R Y_g^i \qquad (1)$$

where Y is peak area corrected for contribution from ^{132m}I and ^{132g}I decay during the irradiation and cooling time.

X is a function involving branching ratio (0.86) in decay of ^{132m}I to ^{132g}I, irradiation time and cooling time. R is a constant inclusive of rate of fission, net detector efficiency and chemical yield.

From least square plot of Y vs X, the ratio $Y_m^i/(Y_m^i + Y_g^i)$ was obtained.

Calculation:

Estimation of Average Angular Momentum From Independent Yield Ratio -

The initial fragment angular momentum distribution was assumed as

$P(J) \propto (2J + 1) \exp [-J(J+1)/B^2]$ where P(J) is the probability of spin J and B is width of the distribution or R.M.S. angular momentum. The initial distribution was corrected for spin change during neutron emission and subsequent dipole gamma emission in cascade so as to obtain the final probability ratio of spin states 8^- (for ^{132m}I) and 4^+ (for ^{132g}I). These calculations were done using Vandenbosch-Huizenga formalism. The parameter B was varied till the experimental independent yield ratio was reproduced. Thus the R.M.S. angular momentum (B) for fragments corresponding to product 132 was obtained.

The independent yield ratio $Y_m^i/(Y_m^i+Y_I^i)$ was obtained as 0.245 ± 0.030 leading to angular momentum value $B = (J^2)^{\frac{1}{2}} = (5.3 \pm 0.3)\hbar$.

5.1.2.3 Calculation of Angular Momenta of Fission Fragments for Various Even-Even Mass Splits in $^{233}U(n_{th},f)$ to Study the Effect of Fragment Deformation

T. Datta, S.P. Dange, Satya Prakash and M.V. Ramaniah

The existing model of Rasmussen et al was modified to take into account of fragment deformation (both quadrupole and octupole). The deformation coefficients α_2 and α_3 were calculated from minimization of potential energy (Deformation energy) for each fragment. Assuming zero point bending mode oscillation only which leads to fragment angular momenta, the bending mode wave function (zero point) was obtained for fragments interacting in strong coulomb field. This bending mode wave function was expanded into spherical harmonics to obtain components of various angular momentum. The obtained distribution

$$a(J) \simeq (2J + 1)\,\gamma^2 \quad \exp\left[-(J + \tfrac{1}{2})^2\gamma^2\right]$$

such that,

$$J_{av} = \frac{\sqrt{\pi}}{2\gamma} - \frac{1}{2}$$

where zero point angular amplitude is given by

$$\gamma^2 = \hbar / (K.\beta)^{\frac{1}{2}}$$

K is the fragment interaction force constant depending on fragment deformation, charge and centre to centre distance. is the bending mode inertial parameter. The experimental kinetic energy distribution data in $^{233}U(n_{th},f)$ and gamma energy for transition between the $2^+ \rightarrow 0^+$ levels in even-even fragment have been used in calculating K & β for each for each fragment in each split.

The calculated angular momenta for fragments as a function of their mass show a saw-tooth behaviour analogous to neutron evaporation curve emphasizing the effect of deformation on bending mode angle (γ) and consequently on angular momentum of the fragment.

5.1.3 Mass Distribution Studies

5.1.3.1 Mass Distribution Studies by Mass Spectrometry

S.A. Chitambar, S.N. Acharya, H.C. Jain and C.K. Mathews

In continuation of the work reported earlier[1,2] for the determination of fission yields of stable and long lived fission products in the thermal neutron fission of ^{233}U, ^{235}U, ^{239}Pu and ^{241}Pu, fission yields of 24 mass numbers from each of the fissioning system have been finalised and compared against the latest compilation by Rider and Meek (NEDO-12154-2E, 1978). All the values are in agreement within 3% except ^{97}Mo, ^{100}Mo and ^{104}Ru in the case of ^{241}Pu where the difference is between 5-17%. Some of the fission yield values in the present work are determined for the first time while only estimates are available in the compilation. Further work is in progress to complete the mass yield curve.

5.1.3.2 Absolute Yields of Short-lived Fission Products in the Thermal Neutron fission of ^{235}U and ^{239}Pu

A. Ramaswamy, V. Natarajan, R. Sampathkumar and R.H. Iyer

Fission product nuclear data such as yields, half-lives, decay schemes, branching ratios etc., are required for the calculation of burn-up, fission products inventories, shielding requirements etc., particularly the short-lived fission products are very much required for decay heat calculations.

We have determined the absolute yields of short-lived fission products with half-lives as low as eight minutes, including some isotopes of krypton in the thermal neutron induced fission of ^{235}U and ^{239}Pu using track etch-cum-gamma ray spectrometric technique. The total number of fission was obtained by track etch technique with an accuracy of 2-3%. The number of fission product atoms was obtained by direct gamma ray spectrometry using a 60cc Ge(Li) coupled to a 4096 channel analyser. A dilute solution of the target material was taken in a sealed polypropylene tube containing a thin mica strip and irradiated along with a tube containing a more concentrated solution of the target material in the pneumatic carrier facility of CIRUS reactor for about half a minute.

After irradiation, the polypropylene tube containing the concentrated target solution was directly mounted on a perspex plate and the gamma counting was done on a precalibrated 60cc Ge(Li) detector coupled to a 4096 channel analyser. The gamma rays spectra were recorded on cassette magnetic tapes and were analysed for different gamma peaks after the end of the entire counting. The analyser system has the facility of automatic peak location and peak area calculation. From the peak area, the disintegration rate of the fission products were obtained by correcting for the gamma abundance and the detector efficiency.

The other tube containing mica detector was cut open and the detector was etched in 40% HF for 30 minutes at room temperature. The fission track developed were counted under an optical microscope. The total number of fissions were obtained from the track density. The details of calculation are given elsewhere[1].

The fission yield values determined are shown in Table (27). The values from recent compilations[2,3] are also included for comparison. The yield value obtained for ^{88}Kr for ^{235}U and ^{239}Pu is lower than the literature values. Since the target was not opened atall after irradiation before the completion of entire gamma counting, the possibility of the escape of rare gases is ruled out. The other possibility is the error in the gamma abundance values used. We have used gamma abundance values from the most recent compilation[4]. Among the different existing compilations, there are slight discrepancies in the reported gamma abundance values for short-lived fission products and hence accurate determination of the same is needed.

Except for the fission products ^{88}Kr and ^{135}I where such discrepancies exist in the gamma abundance values from different compilations, the absolute yields for all others fission products reported are reliable. The maximum overall error is within $\pm$5-6%.

TABLE 27

Absolute yields of short-lived fission products from thermal neutron fission of ^{235}U and ^{239}Pu.

	Sl. No.	Nuclide	$T_{\frac{1}{2}}$	Present determination	Meek and Rider[1]	Crouch[2]
^{235}U	1.	^{85m}Kr	4.5h	1.26 ± 0.01	1.30	1.32
	2.	^{87}Kr	76.3m	2.48 ± 0.12	2.53	2.52
	3.	^{88}Kr	2.8 h	2.86 ± 0.16	3.55	3.55
	4.	^{89}Rb	15.4m	4.44 ± 0.20	4.88*	-
	5.	^{92}Sr	2.71h	6.49 ± 0.09	5.95	5.95
	6.	^{93}Sr	7.3m	6.37 ± 0.04	6.27*	-
	7.	^{104}Tc	18.0m	1.64 ± 0.22	1.82*	-
	8.	^{134}I	53.0m	7.26 ± 0.24	7.61	7.60
	9.	^{134}Te	42.0m	6.80 ± 0.24	6.76	6.69
	10.	^{135}I	6.7h	6.86 ± 0.36	6.30	6.54
	11.	^{138}Cs	32.3m	6.55 ± 0.24	6.72	6.86
	12.	^{142}La	92.0m	5.22 ± 0.09	5.88	5.89
^{239}Pu	1.	^{85m}Kr	4.5h	0.57 ± 0.01	0.55	0.56
	2.	^{88}Kr	2.8h	0.90 ± 0.10	1.33	1.10
	3.	^{89}Rb	15.4m	1.46 ± 0.07	1.70*	-
	4.	^{92}Sr	2.71h	2.87 ± 0.19	2.99*	-
	5.	^{93}Sr	7.3m	3.53 ± 0.20	3.73*	-
	6.	^{104}Tc	18.0m	5.69 ± 0.17	5.95*	-
	7.	^{105}Ru	4.4h	5.42 ± 0.27	5.42	5.48
	8.	^{134}Te	42.0m	4.73 ± 0.16	4.24*	-
	9.	^{135}I	6.7h	7.66 ± 0.46	6.32	5.77
	10.	^{142}La	92.0m	4.36 ± 0.14	4.99	5.00

* Calculated yields.

Many of the yields reported here are determined for the first time experimentally. The values given in literature are from model estimates of the fractional chain yield as a function of the charge of nuclide in the chain.

References

1. R.H. Iyer, R. Sampathkumar and N.K. Chaudhuri, Nucl. Instr. and Methods, 115, 23 (1974).

2. M.E. Meek and B.F. Rider, USAEC Report NEDO-12 154 (1974).

3. E.A.C. Crouch, Atomic and Nuclear Data Tables, 19, 5 (1977).

4. J. Blachot and C. Fiche, Atomic and Nuclear Data Tables, 20, 241 (1977).

5.1.3.3. Yields of Short Lived Fission Products in the Reactor Neutron Induced Fission of ^{238}U.

V.K. Rao, S.G. Marathe, V.K. Bhargava and R.H. Iyer.

A program of work on the measurement of the yields of some short lived fission products in the reactor neutron induced fission of ^{238}U has been initiated. It is proposed to measure the yields of the products with half lives ($t_{\frac{1}{2}}$) less than 30 minutes. The method used for these measurements involves a fast preliminary radiochemical separation of fission products of elements of identical chemical behaviour (i.e. Sr & Ba for example) followed by the track-etch-cum-gamma spectrometric technique developed earlier[1] for the determination of fission yields. In a few irradiations involving Cd-wrapped depleted uranium targets in the pneumatic facility at CIRUS reactor, the yields of ^{141}Ba ($t_{\frac{1}{2}}$=18.3 min), ^{142}Ba (10.7 min), ^{93}Sr (7.45 min) etc. have been obtained.

References

1. S.G. Marathe, V.K. Rao, V.K. Bhargava, S.M. Sahakundu and R.H. Iyer, J. Inorg. Nucl. Chem. 40, 1981 (1978).

5.1.3.4 Studies on Highly Asymmetric Binary Fission

V.K. Rao, V.K. Bhargava, S.G. Marathe, B.K. Srivastava and R.H. Iyer

The work on the Fission Yield determination of some highly asymmetric binary products in the reactor neutron induced fission of ^{238}U has been completed and reported elsewhere[1,2]. One of the

important observations made in these investigations is the appearance of a new shoulder in the highly asymmetric mass region. This has been ascribed to the possible influence of the 38-proton shell.

These studies have now been extended to the thermal neutron induced fission of ^{239}Pu due to the following considerations: (1) Pronounced shell effects leading the occurrence of shoulders are expected at low excitation energies (2) because of higher mass number as compared to ^{235}U, the mass distribution is expected to be broader and the yields in the far asymmetric mass region are expected to be higher making the measurements comparatively easier (3) higher fission cross section for ^{239}Pu than ^{235}U and the absence of ^{239}Np as an activation impurity (in the case of ^{238}U), making the separation of heavier rare earths easier.

Prior to irradiation of Pu targets (which are in the form of sintered oxide), 5 mg amount was taken its dissolution in Conc.HNO_3 containing a few drops of HF was investigated. The time for quantitative dissolution was $\frac{1}{2}$ hr.

One sample containing 5mgs of PuO_2 sealed in quartz tubes was irradiated for 12 hrs in A-1 position of APSARA reactor. The target was dissolved and processed for ^{179}Lu, ^{167}Ho and ^{172}Er in presence of these added carriers using ion exchange separation techniques. The data is being processed at the time of this report.

One of the problems encountered while dissolving the irradiated target was the quantitative dissolution of the target after breaking the quartz ampule containing the irradiated Pu-oxide. Alternative methods for cutting the ampule and dissolution of the target are being planned.

Arrangements for irradiating 3 more targets have been made.

References

1. R.H. Iyer, V.K. Bhargava, V.K. Rao, S.G. Marathe and S.M. Sahakundu, IAEA-SM-241/F 16 (1979).

2. V.K. Rao, V.K. Bhargava, S.G. Marathe, S.M. Sahakundu and R.H. Iyer Phys. Rev C 19, pp 1379-79 (1979).

5.2. Studies on Decay Schemes

A work programme has been started on the study of decay schemes of short-lived radionuclides prepared after fast irradiation and radiochemical purifications. In this direction, the efforts are first concentrated on acquiring the experience on decay schemes of those radionuclides which can be prepared relatively easily and next, extend these studies to radionuclides prepared by fast irradiation, transport and radiochemical purifications. Presently the daughter products of ^{233}U have been chosen for the investigations as they offer some scope of investigation. A considerable amount of experience also is required and will be obtained in these investigations on the associated electronics. A brief description of the work done in these directions are given below. Work at present is in progress on the decay schemes of ^{221}Pr.

5.2.1 Development of a Radiochemical Method for Separation and Purification of ^{221}Fr

A.V.R. Reddy, C.R. Venkatasubramani, S.S. Rattan, Shesha Sayi, V. Mallapurkar, R.J. Singh, Satya Prakash and M.V. Ramaniah

^{233}U which had been prepared a few years earlier was obtained from Fuel Reprocessing Division of BARC. This was used for the preparation of ^{229}Th and its daughter products. The decay series of ^{233}U is shown below.

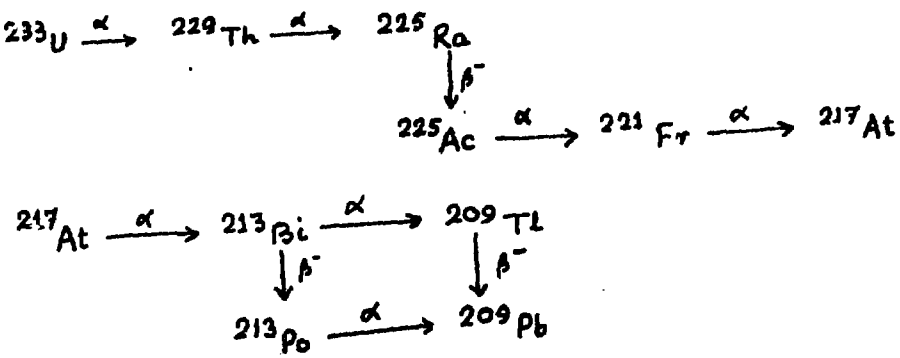

^{229}Th and other daughters were separated from ^{233}U using ion exchange resins Dowex 1 x 8 (200-400 mesh size) Cl^- form. U^{233} and daughters were loaded onto the column in 7M HCl when uranium was held back.

Elution of uranium was done using 0.1M HCl. The purification cycle was repeated twice on fresh columns to completely remove ^{233}U. Separation of ^{225}Ra and other daughters from ^{229}Th was also effected by ion exchange using Dowex 2 x 8, 100-200 mesh, NO_3^- form. ^{229}Th and daughters were loaded onto the column in 7M HNO_3 when ^{229}Th was held back in the column and all daughters came down and collected. Elution of Th was done using 0.1M HNO_3. This purification cycle was also repeated twice.

A series of experiments were conducted to optimise the method of separation and purification of ^{221}Fr as the existing procedure did not give reproducible results and high yields - the yield varying between 30% and 50% of the reported value. The present procedure consists of extraction of ^{225}Ac with an equimolar mixture of TOPO + TTA in benzene at pH 2.5. The extraction time is about 3 minutes. ^{221}Fr is quantitatively milked back in about a minute using pH 7.0 water.

5.2.2 Decay Scheme studies on ^{221}Fr

S.S. Rattan, A.V.R. Reddy, C.R. Venkatasubramani, Satya Prakash and M.V. Ramaniah

Experiments are in progress for the redetermination of the half life of ^{221}Fr. The sample is counted on a 60 cc Ge(Li) detector coupled to a 4K analyser by following the 218 KeV peak of ^{221}Fr in the MCS mode. Gamma ray spectra of ^{221}Fr have been taken to identify the gamma lines of ^{221}Fr by decay and growth. As the experiments involves high counting rates, a correction of pile up at the amplifier stage is necessary for correct half-life estimation. Evaluation of pile-up correction is also under progress.

5.2.3 Calibration of Ge(Li) and Ge Detectors

S.B. Manohar, S.S. Rattan, S.P. Dange, T. Datta, A.V.R. Reddy, C.R. Venkatasubramani, A.G.C. Nair, S.M. Deshmukh, P.P. Burte, V. Mallapurkar, Satya Prakash and M.V. Ramaniah

A calibration of the efficiency of Germanium detectors as a function of the energy of the incident gamma ray is essential for the estimation of radionuclides. Earlier such a calibration had been

accomplished for a 8 cc detector (coupled to a 400 channel analyser). Recently, the Division has acquired a 60 cc Ge(Li) diode, a 2 cc intrinsic germanium diode and a 4K tracer Northern TN-1700 analyser system. Hence, these diodes had to be calibrated.

For the purpose of calibration using standard radio isotopes such as ^{134}Cs, ^{137}Cs, ^{152}Eu, ^{125}Sb, ^{103}Ru, and ^{106}Ru were procured from Laboratories de Metrologie des Rayonnements Unisants, France. Some of these standard radioactivities were recalibrated using the 4 coincidence counting system of this laboratory as a check. The agreement with the quoted value was within one percent. Samples were prepared and counted as the conventional 5 ml liquid solution in standard vials as well as point sources and efficiency as a function of gamma ray energy has been obtained covering a range of energy from 120 to 1700 KeV. The efficiency curve constructed from above multi-isotope standards has an overall accuracy of about 2-3%. Efforts are underway to fit the efficiency curve to a mathematical function as a function of gamma ray energy and evaluation of constants.

5.2.4 Half-Life of ^{242}Pu

S.K. Aggarwal, S.N. Acharya, A.R. Parab and H.C. Jain

The half-life of ^{242}Pu was determined by relative activity method in two independent sets of experiments. The objective was to resolve the discrepancy between the two sets of values available in literature for the half-life of ^{242}Pu measured with reference to ^{239}Pu and ^{236}Pu half-lives and also to obtain the half-life of ^{242}Pu with a high precision and accuracy.

Synthetic mixtures were prepared using enriched isotopes of ^{238}Pu, ^{239}Pu and ^{242}Pu. A new double dilution technique was developed for maintaining the atom ratios and the alpha activity ratios close to unity so that these could be measured with high precision and accuracy. The alpha activity ratios in these mixtures were determined by alpha spectrometry on electrodeposited sources using silicon surface barrier detector while the atom ratios were obtained by mass spectrometry. A half-life value of $(3.742 \pm 0.024) \times 10^5$ yr is

obtained using the half-life of ^{239}Pu as 24110 yr. The value obtained using the half-life of ^{238}Pu as 87.74 yr is $(3.766 \pm 0.025) \times 10^5$ yr. The average of these two independent sets of experiments leads to a half-life value of ^{242}Pu as $(3.754 \pm 0.025) \times 10^5$ yr. The uncertainty given on the values is a combination of one standard deviation on the average value and the error evaluated from estimates on various error components. The discrepancy existing in the earlier published values for the half-life of ^{242}Pu determined relative to the half-lives of ^{239}Pu and ^{238}Pu is resolved. The details of the work are under publication in Physical Review(C).

5.2.5 Half-Life of ^{232}U

S.K. Aggarwal, S.B. Manohar, S.N. Acharya, Satya Prakash and H.C. Jain

The half-life of ^{232}U was determined by two independent methods: specific activity method and a relative activity method involving the half-life of ^{233}U. In the specific activity method, the alpha disintegration rate of ^{232}U was determined by liquid scintillation counting as well as by alpha proportional counting and number of atoms of ^{232}U was determined by isotope dilution mass spectrometry. The radiochemical purity of ^{232}U was confirmed by alpha spectrometry. A half-life value of (69.00 ± 0.40) yr was obtained. In the relative activity method, synthetic mixtures were prepared using isotopes of ^{232}U and ^{233}U. The double dilution technique was employed for maintaining the atom ratios and the alpha activity ratios close to unity so that these could be measured with high precision and accuracy. The alpha activity ratios in these mixtures were determined by alpha spectrometry on electrodeposited sources using silicon surface barrier detector while the atom ratios were obtained by mass spectrometry. A half-life value of (68.61 ± 0.38) yr was obtained using the half-life of ^{233}U as 1.592×10^5 yr. The average of these two independent determinations leads to a value of (68.90 ± 0.39) yr for the half-life of ^{233}U. The uncertainty given on the values is a combination of the one standard deviation on the average value and

the error evaluated from estimates on various error components. The values published earlier are significantly higher as compared to the half-life value obtained in this work. The details of the work are under publication in Physical Review (C).

5.3 Studies on Solid State Track Detectors

5.3.1 Preparation of Nuclepore Filters

R. Sampathkumar and R.H. Iyer

The preparation of Nuclepore Filters was continued with some modifications. The old ^{235}U fission fragment source was replaced by an 1 n.gm. ^{252}Cf source. Since this did not involve time consuming thermal neutron irradiations, the method was simple and direct. The amount of ^{252}Cf source being small, several hours of irradiation was required to produce a single filter. The filters produced in this way had the same characteristics as those produced by thermal neutron irradiation. Filters produced by using ^{235}U source were tested for their filtering properties at Radiation Medicine Centre by filtering diluted human blood through a 4.5μ filters. It was demonstrated that WBCs and RBCs were effectively filtered leaving the colour less plasma as the filtrate.

A 20n.gm ^{252}Cf source would be adequate to prepare one filter per 5 min. Since ^{252}Cf source was not readily available, irradiation with α-particles was tried. Normally alpha particles are not registered easily in polycarbonates since their energy loss rate in polycarbonates is small compared to fission fragments. But it was found that, by adjusting the distance between the source and the detector, alpha particles from ^{237}Np and ^{241}Am were used in the irradiations. Optimum conditions to produce a filter with 10^5 pore density and 0 to 4.2μ pore size were obtained. But the pore size did not increase from 4.2μ even after prolonged etching.

Therefore the possibility of enlarging the pore size by using electric sparks was tried. This method worked but uniform pore size

could not be obtained, pore sizes ranged from 6 to 12μ and the pores were not as circular as obtained by irradiation with fission fragments. It seems, therefore, that ^{252}Cf source is indispensible.

Reference

1. Radiochemistry Annual Report for 1976; BARC 974 (1978) pp 6-7.

5.3.2 Thermal Treatment of Cellulose Nitrate (Daicel) Plastics and Their Effect on Alpha Track Revelation Characteristics.

R. Sampat Kumar and R.H. Iyer

There are different methods to sensitize Daicel, Lexan etc. to reveal full track length of charged particle tracks registered in these materials. Some of the methods are U.V. exposures. γ-ray treatment, heat treatment etc. It has been shown[1]. That a preliminary heating of Daicel for 4 hours at 100-120°C.strongly reduces bulk etching rate increasing the ratio V_T/V_G and therefore favourable for track discrimination.

Heat treatment of Daicel foils were systematically investigated and it turned out that, by heating the foil at 60°C for 7 hours, reduces the bulk etch rate V_G, strongly without affecting the track etch rate, V_T. V_T measurements were carried out by means of a continuous etching process in which the etchant continuously flows in a transparent cells by means of a peristaltic pump. Details of the procedure has been described elsewhere[2].

The track revelation characteristics in any dielectric material for a given etchant depends upon V_G and V_T. The ratio V_G/V_T describes the shape and size of the track. Lesser this ratio, greater is the track length and for ratio equal to one, no track is revealed because the track region is etched as fast as the bulk of the material. By heat treatment V_G is reduced and hence there is an increase in the track length.

By measuring the track lengths in the heated plastic and the unheated one it was shown that shallow pits have reduced by nearly 40% in the heated plastic than that of the unheated one. The enlongated tracks have increased nearly 8 times in the heated plastic

there by increasing the contrast between a track and a non track especially so, for over etched shallow pits. This process has resulted in producing a better detector and also ease in scanning. The results aredepicted in Table 28 where it can be seen, that there is no significant change in V_T for the two types of Daicel. But V_G on the otherhand, changes by a factor 1.81 more for the unheated Daicel. Since V_G and V_T are known, the etching efficiency can be calculated from $\frac{1-V_G}{V_T} = 1 - \sin\theta_c$.

TABLE 28

V_G and V_T measurement data of Daicel.
Etching temperature 32.5°C ± 0.1°C.
NaOH concentration 2.5N. Exposure ^{222}Rn alphas.

Sample	V_G μ/min	V_T μ/min	$1-\frac{V_G}{V_T}$ (%)
Heated	9.3×10^{-3}	0.11	92.5
Unheated	16.8×10^{-3}	0.12	86.0

References

1. M. Nicolae, Proceedings of 8th International Conference on Nuclear Photography and Solid State Track Detectors, Bucharest p.178(1972).

2. R. Sampat Kumar and R.H. Iyer, Radiation Effects Vol.40, Nos.1-2 00 57 to 65.

5.3.3 Alpha Track Registration from Actinides in Solution Medium

B.K. Srivastava, N.K. Chaudhuri, V. Uma, G.R. Mahajan and R.H. Iyer.

In continuation with the studies on alpha track registration from solution medium[1], effects of various factors on the track registration and revelation characteristics were investigated. The measured K_{wet} values of the (a) fission fragments[2], (b) alpha and

^{7}Li ions from ^{10}B (n, ^{4}He) ^{7}Li reaction[3] and (c) alpha particles from actinides have been examined in the light of the range and energy of the charged particle in the medium. Feasibility of utilising the technique for the estimation of uranium or plutonium by track registration from solution medium was demonstarated.

Effect of nitric acid concentration of solution- For short exposure times of the order of a few hours, the values of the K_{wet} factor decreased with increase in the time of exposure in solution containing high concentration of HNO_3. The effect seems to attain saturation after about 7 hrs of exposure in 3N HNO_3 solution. The increase in the bulk rate of detectors exposed in similar conditions also followed a similar trend. When tracks were registered from solution of different nitric acid concentration, solution of different nitric acid concentration, solution below 0-6N seemed to have no effect on the detector material.

Range-energy correlation with the K_{wet} values

From a simple consideration of the geometry of the registration of tracks, the average effective range (R_{eff}) from which a charged particle can produce etchable tracks (R^{av}_{eff}) can be shown to be related to the K_{wet} factor by the relation.

$$K_{wet} = \frac{1}{4} R_{eff} \qquad \text{---------- (1)}$$

For fission and nuclear reactions like ^{10}B (n, ^{4}He) ^{7}Li, where two heavy charged particles are generated, the above equation takes the form of equation[2].

$$K_{wet} = \frac{1}{2} R^{av}_{eff} \qquad \text{---------- (2)}$$

The measured K_{wet} values and the calculated R_{eff} values for average fission fragment and alpha particles from different sources

are given in Table 29. The relative variation of the sinsitivities is reflected in the variation of the values of K_{wet} for different detectors. The value of $R_{eff}^{av}(\sim 18/\mu m)$ as obtained from the measured K_{wet} values by fission track registration are close to but less than the average ranges of the most probable light and heavy fragments ($\sim 20/\mu m$) in water). This small difference may be due to the non etchable portion of the particle range in the detector registration threshold of the detector and the slightly higher density of the aqueous nitric acid medium. The average value of ranges of ^{4}He and ^{7}Li (from reaction of thermal neutrons on ^{10}B) in water are about 7.5 $/\mu m$ for LR 115. The lower values of R_{eff}^{av} obtained with Daicel and CA 80-15 indicate lower sensitivities of these two detectors.

In case of actinide alphas the values of R_{eff} obtained from equation 1 using measured K_{wet} are much less than the range in the medium. For charged particles from fission or $^{10}B(n,^{4}He)\ ^{7}Li$ reaction where the etchable damage starts right from the surface of the detector, the range in the solution medium and the track registration geometry are of primary importance. In case of actinide alphas, however, track revelation efficiency acquires more importance. The etchable regions of the damage trails lie at different depths in the detector material depending on the energy. Within some specified etching time the etchant can reveal only a fraction of the latent tracks (depending on the bulk etch rate) and this fraction is lesser the higher is the energy of the alpha particles. The plateau region in the track density vs time of etching plot is reached when the revelation of new tracks and removal of old tracks due to bulk removal are counter balanced. This is, thus, an upper energy threshold of the alpha particles above which the etchable damage density is embedded at the depth where the etchant does not reach during the optimum time of etching.

The existance of an 'energy window' bounded by a lower and a higher energy thresholds, therefore plays an important role in the alpha track registration from the actinides in the solution medium.

TABLE 29

Measured K_{wet} values and average ranges in water

Track Producing particles	Average range in water in 10^{-4} cm	Detector	Measured K_{wet} values (under optimum etching condition) in 10^{-4} cm	Calculated R_{eff}^{av} in 10^{-4} cm
Fission Fragments from ^{235}U fission	20	Lexan	8.1	16.2
		Melinex-O	8.9	17.8
^{4}He and ^{7}Li from $^{10}B(n,\alpha)^{7}Li$ reaction	7.5	LR-115	3.45	6.9
		CA 80-15	2.25	4.5
		Daicel	2.20	4.4
^{4}He from Uranium (~4.75MeV)	30.6	LR-115	4.15	16.60
		CA 80-15	5.10	20.40
		Daicel	3.40	13.60
^{4}He from Plutonium (~5.16MeV)	35.0	LR-115	5.16	20.64
		CA 80-15	5.71	22.84
		Daicel	2.65	10.60
^{4}He from Americium (~5.48MeV)	38.6	LR-115	3.59	14.36
		CA 80-15	4.48	17.92
		Daicel	3.09	12.33

The track density obtained by alpha track registration from solution medium showed the expected linear relation with the concentration of enriched uranium and plutonium in the solution.

References

1. G.R. Mahajan, V. Uma, B.K. Srivastava, N.K. Chaudhuri and R.H. Iyer. Annual Report, 1977, Radiochemistry Division p.95.

2. R.H. Iyer, R. Sampathkumar and N.K. Chaudhuri, Nucl. Instr. and Meth. 115 (1974) 23.

3. N.K. Chaudhuri, G.R. Mahajan and R.H. Iyer, Nucl. Instr. and Meth, 157 (1978) 545.

5.3.4 Electrochemical Etching of Nuclear Tracks

G.R. Mahajan, N.K. Chaudhuri and R.H. Iyer

When the number of tracks per unit area is very low one has to scan a large area of counting reasonable number of tracks. A large scale amplification of the tracks would enable one to count under low magnification (or even with unaided eye) and reduce the time and labour in scanning. This can be achieved by the chemical etching of the nuclear tracks under the influence of an electric field[1,2]. Generally a function generator is used to produce different wave forms, high frequency and high voltage. This requires a high investment in electronic accessories. Hence, an effort was undertaken to simplify the procedure using mains frequency (50Hz) and a simple high voltage unit. A specially designed teflon cell was fabricated in the divisional workshop. This was placed in a jacketted glass vessel connected to a circulating water bath having thermostatic arrangement. Two stainless steel electrodes were provided-one to be dipped inside the teflon cell and another to be dipped in the solution contained in the glass vessel.

The track detector separates the solution in the cell from the solution in the glass vessel and the leak proofness is ensured by a proper fitting of the screw head using silicone rubber gaskets. Encouraging results had been obtained for fission tracks in polycarbonate films. In the meantime a paper utilising the same type

of set with 50 Hz main supply has been published in literature[3]. However, the electrochemical etching of alpha tracks from actinides using 50 Hz mains supply has not been reported so far and work in this line is in progress. A function generator has been procured for generating different functions and high frequency. Necessary arrangement for stepping up the voltage is being made by the electronic cell of the division before taking up a systematic study of this technique using different detectors.

References

1. L. Pommasino and G. Armellini Rad. Eff. 20, 253 (1973).

2. G. Somogyi, Rad. Eff. 34, 51 (1977).

3. G.M. Nassib and E. Piesch. Nucl. Instr. and Meth. 154, 377 (1978).

5.3.5 Development of Simple Experiments for the Demonstration of Radioactivity Using Solid State Track Detectors

V. Uma, N.K. Chaudhuri and R.H. Iyer

Variation of Energy and Range of Alpha Particles from different nuclides -

Planchetted sources of different nuclides like ^{235}U (enriched uranium), ^{239}Pu, ^{241}Am etc. (which emit alpha particles spontaneously) are separately exposed to alpha sensitive cellulose Nitrate (CN) detector strips (commercially available as Daicel, CA 80-15, LR-115 etc.) kept on the demountable slanting plate (l_3) as shown in the Fig.(11). Tracks would be recorded upto different distances on the detector from the base depending on the energy and hence the range of the alpha particles in air. After exposing for a suitable time (which may be of the order of a few minutes depending on the activity of the planchetted source) the detectors are etched in 2.5 N NaOH solution at 60°C for about 40 minutes, washed in water and then mounted on microscope glass slides. The distance (d) on the detector up to which the tracks are recorded in the detector is measured by viewing through a microscope having a mechanical stage with a vernier scale.

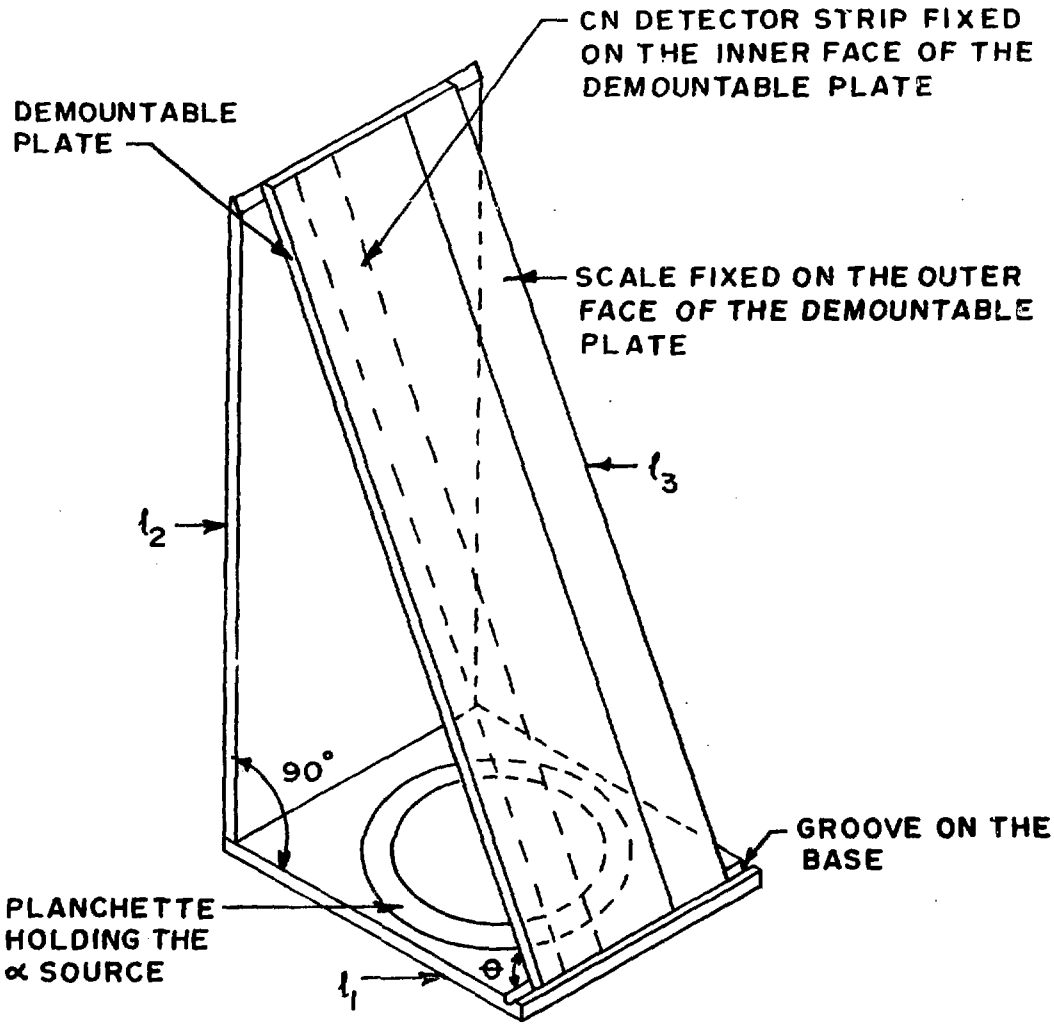

FIG. - II.

Experimental Set-up For Range Measurement in Air

A closed circuit TV coupled to a microscope or a projection microscope with a ground glass screen may be more useful for class room demonstration. The effective range (R_{eff}) of the alpha particles in air is given by $R_{eff} = d \sin\theta$ where θ is the angle of inclination of the detector. Values of R_{eff} thus obtained compares well with range values given in literature. A minimum energy (threshold energy) is required to produce an etchable damage trail in the detector and hence the values obtained by the above procedure is expected to be slightly less than the true range of the alpha particles in air. Nevertheless, these values are good estimates of the true ranges. This simple experiment may be helpful to the teacher not only for demonstrating the existance of alpha activity but also to explain the basic principles for the detection and counting of ionising charged particles. The whole experiment can be conducted within two hours. The frame shown in Fig.(11) can be easily fabricated from plates of metal, plastic, wood or even card board. The angle θ is obtained by measuring the sides of the right angled triangle.

SECTION-6: INSTRUMENTATION

6.1 A Spark Counting Unit

S. Kamaraj, M.R. Ponkshe and J.K. Samuel

A unit to facilitate counting of fission tracks on thin plastic films has been designed. High voltage is applied across the film starting from a low value and then slowly raised. Breakdown of the voltage occurs through the tracks resulting in electrical pulses which are then counted. The unit contains preamplifier, amplifier, discriminator, pulse shaper, scaler and a variable high voltage supply. Its block diagram is given in Fig.(12). The preamplifier has a high impedance FET input and an emitter follower output. This is succeeded by an amplifier with a gain of 20, a milliwolt discriminator and a shaper circuit. The breakdown (spark) pulses, applied to the pre-amplifier input are counted by a four digit scaler with LED display which follows the shaper circuit. The high voltage supply is zener stabilized initially and then shunt regulated to provide a voltage which is continuously variable from 90 V to 1000 V with a 10-turn helipot on the front panel.

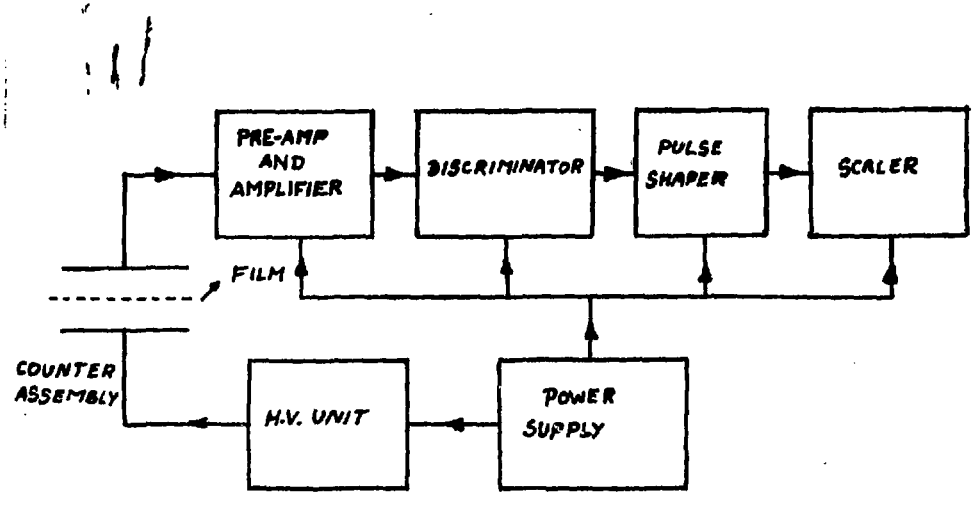

FIG. - 12.

A Block Diagram of Spark Counting Unit

6.2 An Autoranging Alpha Level Monitor

S. Venkiteswaran, M.S. Satsangi and J.K. Samuel

An α- level monitor has been designed and fabricated for use with fractioning columns. The unit monitors α-activity for four seconds, holds the accumulated counts for the next one second, then resets itself and starts again. Its digital display has ranges from 0 to 9.9×10^5 counts in autoranging mode and consists of five seven segment LED digits, the first three showing three most significant digits with a decimal point after the first digit the fourth denoting the letter E permanently and the fifth displaying the value of exponent which can vary from 2 to 5. The circuiting is such that when the count exceeds the range, it automatically switches over to the next higher range. The block diagram of the system is shown in Fig.13.

The detector probe of the system incorporates a 50 mm^2 silicon surface barrier detector and a preamplifier inside a cylindrical housing and is connected to the main unit with a single co-axial cable. Signal from the probe is amplified and fed to counting decades through a comparator, shaper and various controlling gates. Timing signal is generated for repetitive count (4 Sec.) - hold (1 Sec.) sequence. Gates select the number of decades in different ranges, change the display of exponent and provide reset and start pulses. An audible alarm which sounds as soon as the counts overflow the lowest range, is specially incorporated so that the experimentor is alerted to the level of activity in the fraction which has at that time exceeded the background level.

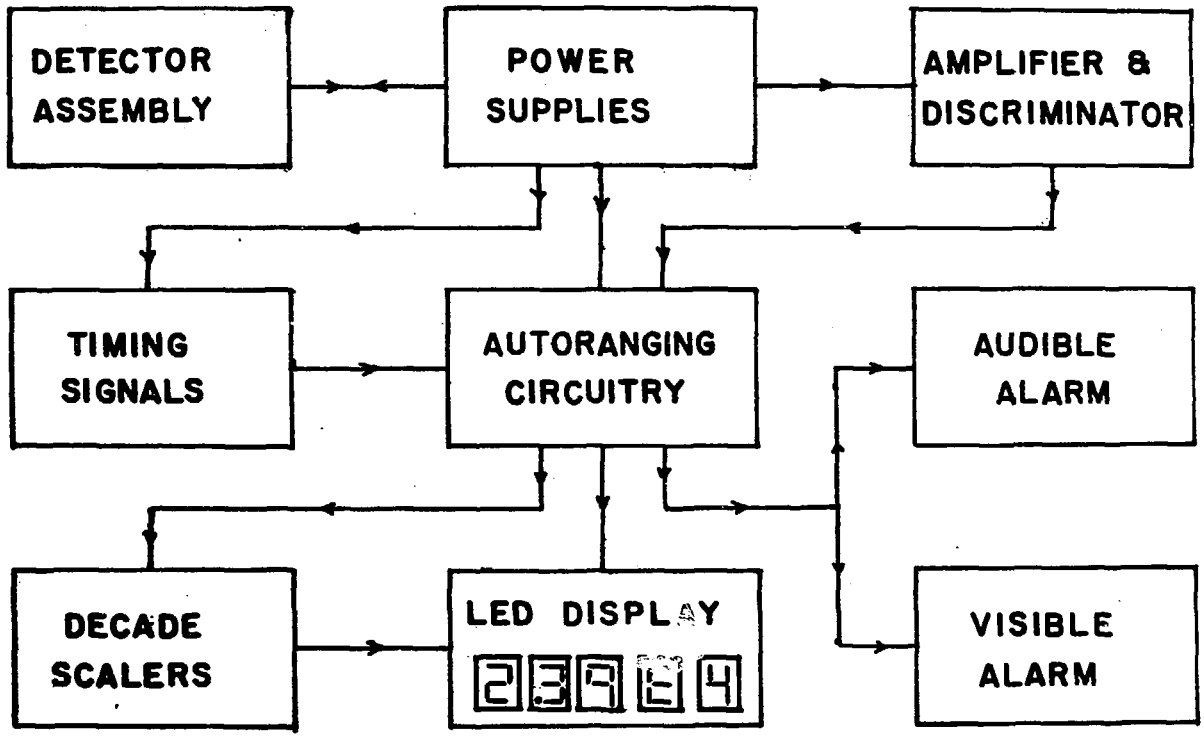

FIG.-13.

A Block Diagram of an Autoranging Alpha-Level Monitor

6.3 Fabrication and Calibration of a Remote Pipetter

C.K. Sivaramakrishnan, A.V. Jadhav, K. Raghuraman, K.A. Mathews and P.S. Nair

A 750 µl. capacity remote pipetter for use in hot cells was fabricated indigenously in our division. This consists of a teflon syringe with a S.S. Piston. The piston is driven by a stepper motor. The motor is coupled through a helipot for controlling the displacement. The remote pipetter was calibrated with uranium solution with predetermined density. Number of 50, 100, 250, 500, 750 µl. volumes were delivered and the exact volume of the solution delivered was calculated by weighing the solution in a Mettler balance. The accuracy for 100-750 µl deliveries was better than 0.5%.

6.4 Indigenous Fabrication of Master Slave Manipulators

C.K. Sivaramakrishnan, A.V. Jadhav

One member of the group participated in testing of master slave manipulators fabricated indigenously by M/s. Visual Education Aids, Coimbatore and M/s. Jayshree Industries, Secunderabad. Several modifications were suggested and incorporated to improve the performance of these master slave manipulators.

6.5 Use of Nova 3/12 Computer Coupled To TN-1700 Multichannel Analyser

S.S. Rattan, A.V.R. Reddy, C.R. Venkatasubramani, T. Datta, A.G.C. Nair, P.P. Burte, S.P. Dange, S.B. Manohar and Satya Prakash.

The TN-1700 multichannel analyser is based on NOVA 3/12 mini computer which can be used independent of the analyser. The language used is a modified version of BASIC, incorporating number of features which allow interaction with the analyser. All types of arithmetic operations and mathematical functions commonly used are available.

The interaction of the programmer with the analyser in through the teletype. The programs after debugging can be stored on magnetic cassettes or paper-tapes for further use.

The following programmes have been developed and run successfully on this computer.

1. Determination of half-life of a given radionuclide from the given decay date with time correction using the method of least square fitting.
2. To convert the date of the counting carried out in LIST mode into PHA mode.
3. To process the spectra of the counting carried out in LIST mode with the help of two parameter routes for fission X-rays and fission fragments which are in coincidence. In this program any number of spectra stored in the magnetic cassette can be analysed in one run.
4. To find the (a) mean and standard deviation for a given set of values (b) least square fitting of given data to the equations.
   i) $Y = mx + c$
   ii) $Y = ax^2 + b\,x + c$
5. Solution of quadratic and trancedental equations.
6. Solution of determinants and various Matrix operations.
7. Plotting of given data in linear or semiloog scale on Teletype.
8. Plotting and displaying the data on oscilloscope.
9. Mapping of the following mathematical functions :- circle, parabola, hyperbola and ellipse.

6.6 A Versatile Thermoluminescence Unit for Radioactive Samples

A.G.I. Dalvi, M.D. Sastry and B.D. Joshi

Thermally stimulated luminescence normally referred to as thermoluminescence (TL) is known to contribute significantly to the understanding of luminescent processes in solids. To study the radioactive recombination and self activation processes in inorganic materials with radioactive elements as activators, a versatile thermoluminescence (TL) unit, adapted for glovebox operation, has been designed

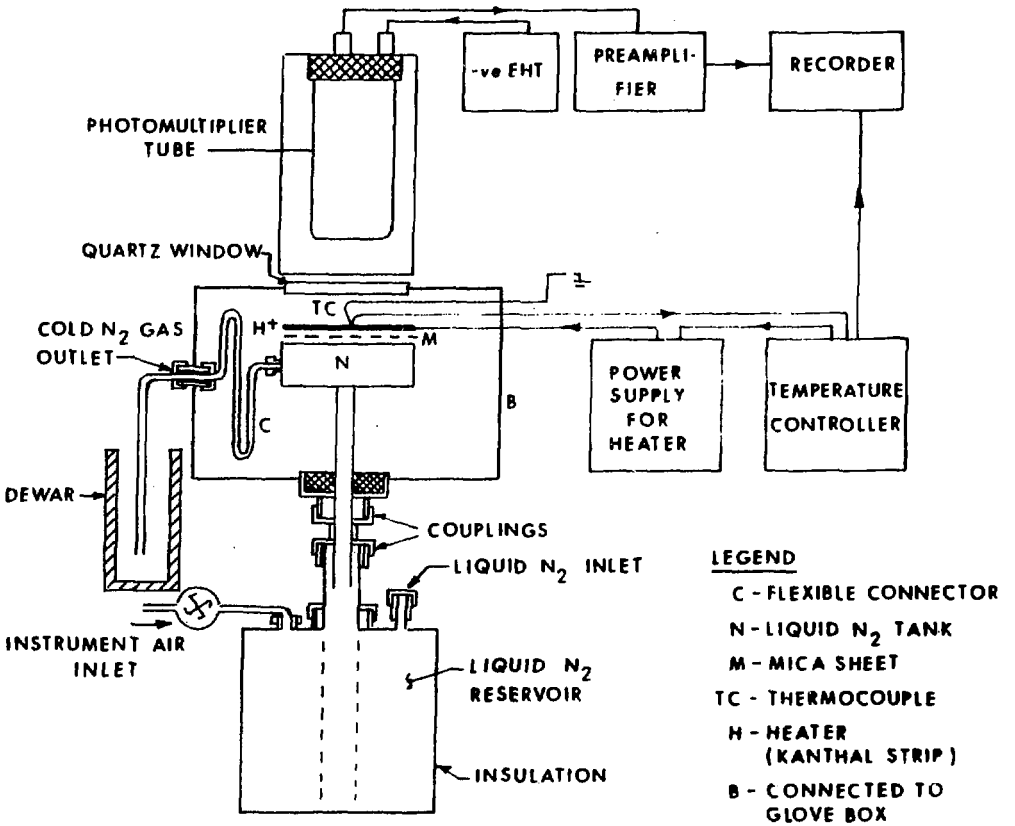

FIG.-14.

A Block Diagram of Thermoluminescence Unit for Radioactive Samples

and fabricated. The unit has provision to record the TL output in two temperature ranges 100-320°C and 300-750°K. The unit incorporates an electronic temperature programmer which can control the rise in temperature of a kanthal strip at constant heating in the ranges mentioned above. The salient features of the instrument include five linear heating rates viz., 0.1, 0.25, 0.5, 1.0 and 2.5°K sec. and facility to maintain the temperature of the sample for a long time within $\pm$ 1°C at any desired value in the two ranges, to enable isothermal decay studies. Furthermore, the unit has the advantage of attaining the lower temperatures (100-320°K range), without the cryogenic liquid (liquid N_2) or cooled gas directly coming into contact with the sample thereby avoiding radioactive contamination of the evaporating liquid. Figures 14 and 15 show the block diagram and a photograph of the TL unit respectively. Glow curves for the standard phosphors viz. CaF_2, TLD-100 and Dy: $CaSO_4$, obtained in both temperature ranges are found to be in good agreement with those reported in the literature.

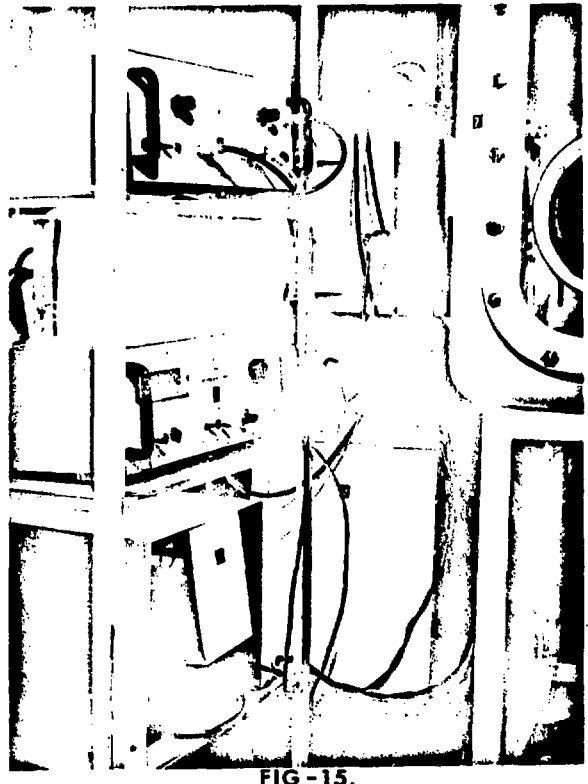

FIG-15.
A Photograph of Thermoluminescence Unit

List of Publications during 1978

(Papers published in Journals, Reports, presented at Conference/Symposia and Theses)

1. Extraction of Plutonium (IV), Uranium (VI) and Some Fission Products by Di-n-Hexyl Sulphoxide
S.A. Pai, J.P. Shukla, P.K. Khopkar and M.S. Subramanian
J. Radioanal. Chem. 42, 323 (1978).

2. Gravimetric Determination of Carbon in Uranium Carbide
V.K. Manchanda and M.S. Subramanian
Fresenius, Z. Anal. Chem., 290, 302 (1978).

3. Extractive Photometric Determination of Plutonium (IV) with Aliquat-336 and Xylenol Orange
J.P. Shukla and M.S. Subramanian, J. Radioanal. Chem. 47, 29 (1978).

4. Studies of HTTA extraction of Tetravalent Actinides
A. Ramanujam, M.N. Nadkarni, V.V. Ramakrishna and S.K. Patil
J. Radioanal. Chem. 42, 349 (1978).

5. A Spectrophotometric method for the determination of Np and Pu in process solutions.
P.R. Vasudeva Rao and S.K. Patil
J. Radiaanl. Chem. 42, 399 (1978).

6. Sulphate Complexing of some trivalent Actinides
P.R. Vasudeva Rao, S.V. Bagawde, V.V. Ramakrishna and S.K. Patil
J. Inorg. Nucl. Chem. 40, 123 (1978).

7. Thiocyanate Complexing of Np(IV) and Pu(III)
P.R. Vasudeva Rao, S.V. Bagawde, V.V. Ramakrishna and S.K. Patil
J. Inorg. Nucl. Chem. 40, 339 (1978).

8. Aqueous Coordination Complexes of Neptunium
S.K. Patil, V.V. Ramakrishna and M.V. Ramaniah
Coord. Chem. Rev. 25, 133 (1978).

9. Nitrite Complexing of Am(III) and Cm(III)
P.R. Vasudeva Rao, M. Kusumkumari and S.K. Patil
Radiochem. Radioanal. Letters 33, 305 (1978).

10. The Effect of Temperature on the Extraction of Pu(IV) by TBP
A. Ramanujam, V.V. Ramakrishna and S.K. Patil
J. Inorg. Nucl. Chem. 40, 1167 (1978).

11. Effect of temperature on the extraction of U(VI) from nitric acid by TBP. S.V. Bagawde, P.R. Vasudeva Rao, V.V. Ramakrishna and S.K.Patil
J. Inorg. Nucl. Chem. 40, 1913 (1978).

12. Absorption Spectra of Np(V) in Aqueous Solutions
P.R. Vasudeva Rao and S.K. Patil
Radiochem. Radioanal. Letters 36, 169 (1978).

13. Solvent Extraction of Tm(III) by Sulphoxides and mixtures of DPSO and HTTA from perchlorate and thiocyanate media.
V.V. Ramakrishna, S.K. Patil, L. Krishna Reddy and A.S. Reddy
J. Radioanal. Chem. 47, 57(1978).

14. Determination of Cd and Li in U_3O_8 powder by AAS with carbon cup atomization
A.G. Page, S.V. Godbole, Sandhya B. Deshkar and B.D. Joshi
Anal. Letters 11, 619 (1978).

15. Determination of refractory elements in U_3O_8 by carrier distillation emission spectrography.
A.G.I. Dalvi, C.S. Deodhar, T.K. Sheshagiri, Medha S. Khalap and B.D. Joshi
Talanta 25, 665 (1978).

16. Application of Track Registration Technique in the estimation and fissile Materials: Analysis of Uranium in Rock Samples.
G.R. Mahajan, N.K. Chaudhuri, R. Sampathkumar and R.H. Iyer.
Nuclear Instruments and Methods 153 (1978) 253-257.

17. EPR Study of Sodium Plutonyl acetate $NaPuO_2(CH_3COO)_3$ and plutonium thenoyl trifluoroacetonate $Pu(TTA)_4$: Self-irradiation effects.
M.V. Krishnamurthy
Radiochem. Radioanal. Letters. 34, 331-338 (1978).

18. Absolute yields of ^{99}Mo and ^{111}Ag in the reactor neutron induced fission of ^{238}U.
S.G. Marathe, V.K. Rao, V.K. Bhargava, S.M. Sahakundu and R.H. Iyer.
J. Inorg. Nucl. Chem. 40, 1981 (1978).

19. Nuclear track registration in solid state track detectors immersed in solutions: Determination of Boron in Complex Matrices.
N.K. Chaudhuri, G.R. Mahajan and R.H. Iyer
Nucl. Inst. Methods. 157, 545 (1978).

20. Separation of heavier rare earths from neutron irradiated uranium targets
V.K. Bhargava, V.K. Rao, S.G. Marathe, S.M. Sahakundu and R.H.Iyer
J. Radioanal. Chem. 47, 5 (1978).

21. Charge distribution in nuclear fission: Determination of fractional cumulative yield of ^{134}Te and ^{135}I in the spontaneous fission of ^{252}Cf.
S.B. Manohar, T. Datta, S.S. Rattan, Satya Prakash and M.V.Ramaniah
Phys. Rev. C-17, 188 (1978).

22. Thermodynamic study of Mg + Bi alloys by vapour pressure measurement using transpiration techniques.
Rajendra Prasad, V. Venugopal and D.D. Sood
J. Chem. Thermodynamics, 10, 135 (1978).

23. The vaporisation thermodynamics of uranium tetrachloride
Ziley Singh, Rajendra Prasad, V. Venugopal and D.D. Sood
J. Chem. Thermodynamics, 10, 129 (1978).

24. An Isoperibol Solution Calorimeter for Heating Reactions
V.K. Manchanda, M.R. Ponkshe and M.S. Subramanian
BARC Report, 989 (1978).

25. Formation of Secondary Amine in the Radiolysis of trilaurylamine
P.K. Bhattacharyya, R. Veeraraghavan and P.B. Ruikar
BARC Report-982 (1978).

26. Spectrochemical determination of trace metals in uranium
T.R. Bangia, Kum. Mary John, V.A. Raman and B.D. Joshi
BARC Report-950, (1978).

27. Determination of plutonium-241 in plutonium using gas flow proportional counter
S.K. Aggarwal, N.K. Porwal, A.R. Parab and H.C. Jain,
BARC Report I-479 (1978).

28. Mass spectrometric analysis of lithium.
S.A. Chitambar, V.D. Kavimandan, S.K. Aggarwal, P.M. Ramasubramanian
P.M. Shah, A.I. Almoula, S.N. Acharya, A.R. Parab, H.C.Jain,
C.K. Mathews, and M.V. Ramaniah
BARC Report-976 (1978).

29. A temperature programme and control unit
J.B. Mhatre, M.R. Ponkshe and J.K. Samuel
BARC Report-I/499 (1978).

30. Radiochemistry Division Annual Report for 1976.
R.H. Iyer (Ed)
BARC Report-974 (1978).

31. A passive gamma scanner for estimation of plutonium in fabrication waste.
P.P. Venkatesan, P.P. Burte, S.B. Manohar, Satya Prakash and
M.V. Ramaniah
BARC Report-986 (1978).

32. Solvent extraction of Plutonium (IV), Uranium (VI) and some fission Products by Di-n-octylsulphoxide
S.A. Pai, J.P. Shukla and M.S. Subramanian
Convention of Chemists, Waltair (1978).

33. The Isolation of Ovotransferrin and Studies on its Complex Formation with Tetravalent Plutonium and Cerium.
I.K. Oommen and M.S. Subramanian
Convention of Chemists, Waltair (1978).

34. Spectrophotometric Study of the adduct formation between $U(TTA)_4$ with some neutral ligands
A. Ramanujam, V.V. Ramakrishna and S.K. Patil
Convention of Chemists, Waltair (1978).

35. Solvent Extraction Studies on Uranium and Plutonium from Phosphoric acid
R. Thiagarajan, R. Swarup and S.K. Patil
Convention of Chemists, Waltair (1978).

36. Structural and thermal studies on chromium-uranium-oxygen system.
A. Chadha, S. Sampath and D.M. Chackraburtty
Convention of Chemists, Waltair, (1978).

37. Graphite furnace atomic absorption spectrometric studies of Eu, Dy, Er and Sm separated from uranium
M.D. Sastry, M.K. Bhide, K. Savitri, Y. Babu and B.D. Joshi
Convention of Chemists, Waltair, (1978).

38. Direct determination of copper and potassium in uranium by furnace atomization atomic absorption spectrometry
B.M. Patel, Neelam Gupta, Paru Bhatt, and B.D. Joshi
Convention of Chemists, Waltair, (1978).

39. Spectrographic determination of twenty-three metallic impurities in uranium using Ga_2O_3+SrF_2
A.G. Page, S.V. Godbole, Madhuri J. Kulkarni and S.S. Shelar
Convention of Chemists, Waltair, (1978).

40. Thermoluminescence and electron spin resonance of europium doped $SrSO_4$ phosphor
A.G.I. Dalvi, C.S. Deodhar and M.D. Sastry
Convention of Chemists, Waltair, (1978).

41. Anion exchange separation and purification of neodymium from fission products
K.L. Ramakumar, V.A. Raman, P.S. Khodade and H.C. Jain
Convention of Chemists, Waltair, (1978).

42. Flameless AAS and its applications in direct assay of metallic elements in uranium
B.M. Pate, Convention of Chemists, Waltair, (1978).

43. Nitrate and Sulphate Complexing of Trivalent Americium, Curium and Californium
P.K. Khopkar and J.N. Mathur
Convention of Chemists, Waltair (1978).

44. Extraction of Trivalent actinides and Lanthanides by a long chain Quaternary Amine
P.K. Khopkar and J.N. Mathur
Convention of Chemists, Waltair (1978).

45. Stability of Constants of Plutonium(III) Complexes with some carboxylic acids
G.M. Nair and J.K. Joshi
Convention of Chemists, Waltair, December (1978).

46. Determination of Uranium and Plutonium in binary mixtures using nuclear track registration from solution medium
G.R. Mahajan, V. Natarajan, N.K. Chaudhuri and R.H. Iyer
Convention of Chemists, Waltair (1978).

47. Thermodynamics of the vaporisation of thorium tetraiodide
Ziley Singh, V. Venugopal, Rajendra Prasad and D.D. Sood
Convention of Chemists, Waltair, (1978).

48. Sol-gel process for ceramic nuclear fuels - Preparation of UO_2-ThO_2 microspheres
V.N. Vaidya, R.V. Kamat, J.K. Joshi, V.S. Iyer, N.L. Srinivasan, K.T. Pillai and D.D. Sood
Convention of Chemists, Waltair, (1978).

49. Physico-chemical studies in condensed media using VEC
D.M. Chakrabortty, P.K. Bhattacharyya, R.D. Saini and K.D. Sigh Mudher
Seminar on Chemistry Research using Cyclotron
BARC, Bombay, (March 22, 1978).

50. Thermoluminescence unit for radioactive samples in the temperature range 100-750°K.
A.G.I. Dalvi, M.D. Sastry and B.D. Joshi
DAE Symposium on Solid State and Nuclear Physics (1978).

51. Selection rule in β-decay of ^{209}Tl
S.N. Acharya, C.V.K. Baba, S.K. Bhattacharjee, S.A. Chitambar V.M. Datar, H.C. Jain and C.S. Warke
DAE Symposium on Solid State and Nuclear Physics, Bombay (1978).

52. Absolute yields of short lived fission products in the neutron fission of Actinide Isotopes.
A. Ramaswamy, V. Natarajan, R. Sampathkumar and R.H. Iyer
DAE Symposium on Solid State and Nuclear Physics, Bombay (1978).

53. Angular momentum in fission: Average angular momentum of fission fragments in the thermal neutron induced fission of ^{233}U.
T. Datta, S.P. Dange, A.G.C. Nair, Satya Prakash and M.V. Ramaniah
DAE Symposium on Solid State and Nuclear Physics, Bombay (1978).

54. Mass spectrometric analysis of uranium and plutonium and its applications in nuclear fuel cycle
H.C. Jain
Proceedings of the seminar on mass spectrometry - Applications and current trends, BARC, Bombay, March 20-22 (1978), p.55

55. The applications of thermal ionisation mass spectrometry in nuclear technology,
C.K. Mathews
ibid, p.41.

56. Isotopic analysis of lithium, boron and magnesium and their importance in nuclear technology
S.A. Chitambar, S.K. Aggarwal and B. Saha
ibid, p.62.

57. On-line data acquisition and processing system for isotope abundance measurements using a mass spectrometer,
S.K. Aggarwal, B. Saha, C.K. Mathews, D. Ranga Rao and Dilip Kumar
ibid, p.165.

58. In-line instrumentation in nuclear fuel reprocessing plants
V.K. Bhargava, V.K. Rao, S.G. Marathe and R.H. Iyer
Symp. on appliction of radioisotopes in chemical and metallurgical industries, Bombay (1978).

59. Physico-chemical studies on the complexes of Plutonium(III) and Americium (III)
Keshav Chander
M.Sc. Thesis, University of Bombay (1978).

60. Determination of the Stability Constants of the Complexes of Plutonium(III) and Samarium (III)
J.K. Joshi
M.Sc. Thesis, University of Bombay (1978).

61. Isolation of a Body Fluid Protein and Studies on its Complex Formation with Plutonium, Cerium and Iron
Isaac K. Commen,
M.Sc. Thesis, University of Bombay (1978).

62. Spectrochemical Methods of Trace Analysis
B.M. Patel,
Ph.D. Thesis, University of Bombay (1978).

63. The chemistry of Actinide Elements - Complex Formation and Solvent Extraction Studies, S.V. Bagawde,
Ph.D. Thesis, University of Bombay (1978).

64. The chemistry of Actinide Elements - Studies on Complex Formation by Solvent Extraction and Spectrophotometry,
P.R. Vasudeva Rao, Ph.D. Thesis, University of Bombay (1978).